

**Hydroxyapatite Deposition on Polypeptide  
under a Condition  
Mimicking Body Environment**

**Akari Takeuchi**

**2006**

**Graduate School of Materials Science  
Nara Institute of Science and Technology**

# ***Contents***

---

<b><i>General Introduction</i></b> .....	1
--	---

## ***Chapter 1***

Formation of Hydroxyapatite on Silk Fiber in a Solution Mimicking Body Fluid .....	23
---	----

## ***Chapter 2***

Formation of Hydroxyapatite on Silk Sericin in a Solution Mimicking Body Fluid: Structural Effect of Sericin .....	45
---	----

## ***Chapter 3***

Formation of Hydroxyapatite on Synthetic Polypeptide in a Solution Mimicking Body Fluid .....	59
--	----

<b><i>General Summary</i></b> .....	87
-------------------------------------	----

<b><i>Publication List</i></b> .....	91
--------------------------------------	----

<b><i>Acknowledgements</i></b> .....	95
--------------------------------------	----

# ***General Introduction***

Bone is one of essential organs, which has various functional properties including structural support, protection of organs, and mineral ion homeostasis [1]. It is sometimes damaged because of disease, injury or aging. When the damage is small, it can be repaired due to the natural healing properties of bone. However, when the damage is large, it cannot be repaired naturally and surgical treatment is needed to replace the missing bone with a substitute. Although autografts and allografts are commonly used as substitutes, there are various problems with these materials such as limited supply, immune response and the risk of infections. In order to overcome the limitations of autografts and allografts, artificial materials have been used as bone grafts. Artificial materials implanted into a bone defect are, however, generally recognized as foreign and thus encapsulated by a fibrous tissue layer of collagen [2]. This is a normal reaction to protect our body from foreign substances. As a result of this, the material implanted into the bone defect is isolated from the surrounding bone and does not bond to the living bone directly.

In the early 1970's, Hench *et al.* [3-5] discovered that some glasses in the  $\text{Na}_2\text{O-CaO-SiO}_2\text{-P}_2\text{O}_5$  system were able to directly bond to living bone without a fibrous tissue layer forming around them. Since the discovery of these glasses, named Bioglass<sup>®</sup>, several ceramics that have bone-bonding ability have been

## General Introduction

---

developed. For instance, sintered hydroxyapatite ( $\text{Ca}_{10}(\text{PO}_4)_6(\text{OH})_2$ ) [6, 7], glass-ceramics containing crystalline apatite (Ceravital<sup>®</sup>) [8], and glass-ceramics containing crystalline oxyfluoroapatite and wollastonite (Cerabone<sup>®</sup> A-W) [9,10] can also directly bond to living bone. When these materials are implanted into bone defects, they form a hydroxyapatite layer on their surface and bond to living bone through this layer [11]. The formed hydroxyapatite is quite similar to hydroxyapatite in living bone in terms of composition and crystallinity, and is therefore often referred to as a bone-like apatite.

In order to reproduce the hydroxyapatite formation on the materials in the living body, Kokubo *et al.* [12] proposed a simulated body fluid (SBF). SBF is a protein-free and acellular aqueous solution with ion concentrations nearly equal to

**Table 1.** Ion concentrations of simulated body fluid (SBF), and human plasma

Ion	Concentration / mM	
	Human plasma	SBF
$\text{Na}^+$	142.0	142.0
$\text{K}^+$	5.0	5.0
$\text{Mg}^{2+}$	1.5	1.5
$\text{Ca}^{2+}$	2.5	2.5
$\text{Cl}^-$	103.0	147.8
$\text{HCO}_3^-$	27.0	4.2
$\text{HPO}_4^{2-}$	1.0	1.0
$\text{SO}_4^{2-}$	0.5	0.5



that of human blood plasma as shown on Table 1. When materials that have bone-bonding ability are soaked in SBF, they form a hydroxyapatite layer on their surfaces.

The property that allows materials to bond to living bone, defined as a bioactivity, is attractive for achieving long-term fixation of the materials. Therefore, materials, such as Bioglass<sup>®</sup>, sintered hydroxyapatite and some glass-ceramics, have been used as periodontal fillers, bone fillers, iliac crests, artificial vertebrae, and intervertebral discs in the orthopedic field. However, their mechanical properties limit their clinical use as they have lower fracture toughness and a higher elastic modulus than human bone [13]. Therefore, the development of the materials with bioactivity and high fracture toughness is also expected. Recently, it has been shown that titanium, titanium alloy and tantalum can be provided with bioactivity through chemical treatment with sodium hydroxide solution, followed by heat treatment [14-22] or treatment with hydrogen peroxide containing various kinds of metal salts [23]. These metallic materials show bioactivity as well as higher fracture toughness than conventional bioactive ceramics. However, they also have higher elastic moduli than cortical bone, which may cause resorption of the surrounding bone due to stress shielding effects.

Bone is a hybrid composed of 22 wt% organic matrix and 69 wt% hydroxyapatite. Hydroxyapatite in bone differs from sintered stoichiometric hydroxyapatite: it is usually calcium-deficient and carbonate-substituted apatite with low crystallinity [7]. It is formed as needle-like crystals, with 20-40 nm in length and with 1.5-3 nm in thickness, in collagen fiber matrix by a biomineralization process. These hydroxyapatite-containing collagen fibers are arranged into a higher ordered organization and result in the anisotropic structure of bone shown in Figure

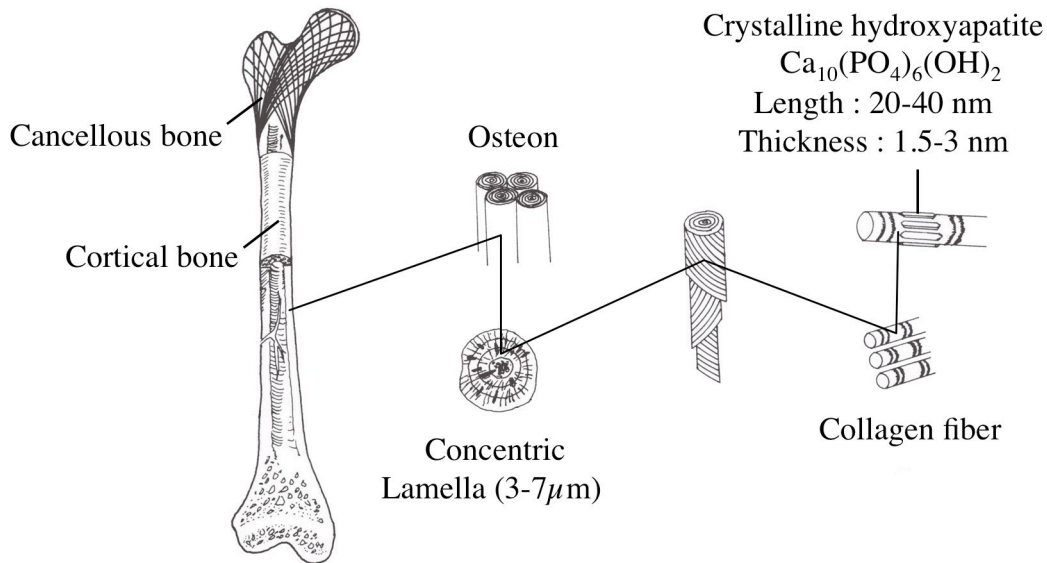


**Figure 1.** Structure of bone. [26]

1 [24-26]. This unique structure of bone provides excellent mechanical properties, such as high fracture toughness and low elastic modulus, and allows bone to bear stress.

Lessons from the natural bone structure are useful for designing novel materials: a material consisting of hydroxyapatite and an organic polymer is believed to be a candidate for bone substitution. Bonfield *et al.* [27,28] first developed a material consisting of hydroxyapatite and an organic polymer: a composite of hydroxyapatite granules and high-density polyethylene. This composite, called HAPEX<sup>®</sup>, is clinically used in middle ear devices. It loses deformability when the hydroxyapatite content exceeds 40 vol%. When the hydroxyapatite content is reduced to less than 40 vol%, however, the composite cannot show high bioactivity because most of the hydroxyapatite granules are embedded in the polyethylene matrix [4].

Coating of hydroxyapatite also provides materials composed of hydroxyapatite and organic polymers. Hydroxyapatite coatings onto materials have been achieved by methods such as plasma splaying, electrostatic deposition, hot isostatic pressing (HIP'ing), ion beam sputtering and radio beam sputtering. The formation of hydroxyapatite through these methods, however, requires treatment at high temperature in or after the process of hydroxyapatite deposition. Therefore, it is impossible to apply these coating methods to hydroxyapatite coating of organic polymers.

Hydroxyapatite found in bone is produced spontaneously in a physiological environment at low temperature from body fluid, since the body fluid is already supersaturated with respect to hydroxyapatite under normal conditions [29,30]. In order to apply this process, in which hydroxyapatite is produced in the body environment, to hydroxyapatite coating, deposition of hydroxyapatite from aqueous solutions has focused attention of many researchers in recent years [31-39]. This method is particularly suitable for coating polymeric materials [31-36], because it can be carried out under ambient conditions. Kokubo *et al.* [31] first proposed a biomimetic process in which a hydroxyapatite layer was coated onto the surface of a substrate using SBF. Figure 2 shows a diagram of the coating procedure through this process. The biomimetic process consists of two steps: hydroxyapatite nucleation and growth of the nuclei. A substrate is first soaked in SBF in contact with CaO-SiO<sub>2</sub> based glass particles. Silicate ions are released from the glass particles and adsorbed on the substrate to induce formation of hydroxyapatite nuclei [32,39,40]. The substrate is subsequently soaked in another solution, such as SBF or a more saturated solution. Hydroxyapatite nuclei, formed on the substrate surface in the initial step, spontaneously grow into a hydroxyapatite layer consuming

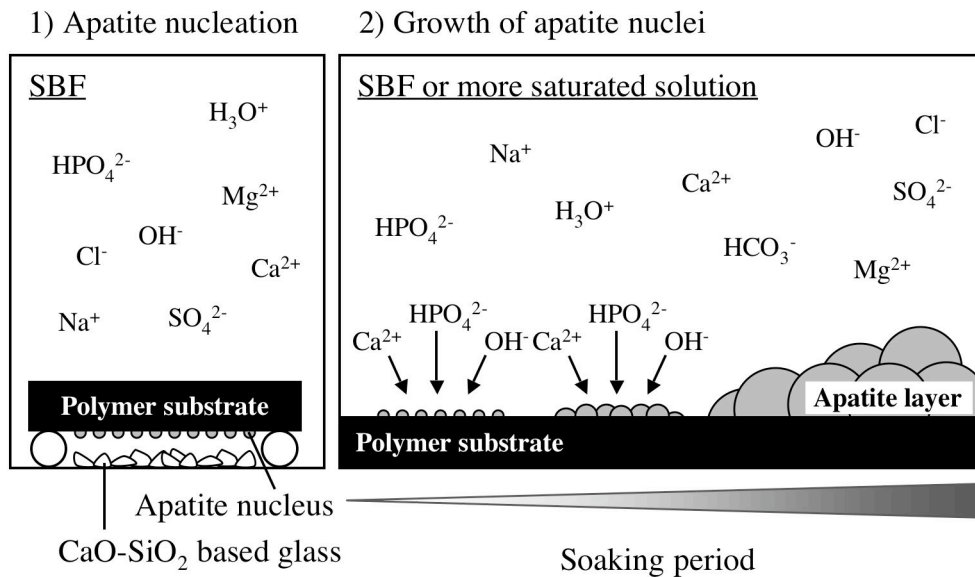


**Figure 2.** Diagram of the biomimetic process proposed by Kokubo *et al.* [32] for coating a polymer substrate with hydroxyapatite.

surrounding ions because SBF is supersaturated with respect to hydroxyapatite even under normal conditions. The hydroxyapatite layer formed through this process consists of a carbonate-containing hydroxyapatite with small crystallites and a defective structure, it shows a high biological affinity when implanted into bone defects, and can bond tightly to living bone. [41]. However, the problem with this process is that the hydroxyapatite layer is only coated on the surface faced on glass particles. If nucleation of hydroxyapatite is induced more effectively, the hydroxyapatite layer would be deposited on the whole surface of the organic polymer substrate.

Investigations into hydroxyapatite formation have demonstrated that hydroxyapatite nucleation on material surfaces in SBF are induced by specific functional groups. Since the reports that -SiOH groups induce the formation of

hydroxyapatite nuclei [42-45], some functional groups other than -SiOH group, that can induce the formation of hydroxyapatite nuclei, have also been reported. The functional groups, such as -TiOH [46-48], -ZrOH [49], -TaOH [50] and -NbOH [51], induce hydroxyapatite nucleation on the surfaces of metal oxide gels, and -COOH, -OPO<sub>3</sub>H<sub>2</sub> and -SO<sub>3</sub>H groups induce it on polymer surfaces [52,53]. The mechanism of hydroxyapatite formation on substrates with those functional groups has also been investigated: the nucleation of hydroxyapatite is initiated by incorporation of Ca<sup>2+</sup> ions into those functional groups on the substrate surfaces, and then HPO<sub>4</sub><sup>2-</sup> and OH<sup>-</sup> ions subsequently bind to the positive surface, as shown in Figure 3. Once hydroxyapatite nuclei are formed, they spontaneously grow into the hydroxyapatite layer.

Many attempts to coat a hydroxyapatite layer onto the surfaces of various substrates containing functional groups that induce hydroxyapatite nucleation have been made in recent years, using a biomimetic process [54-59]. The majority of

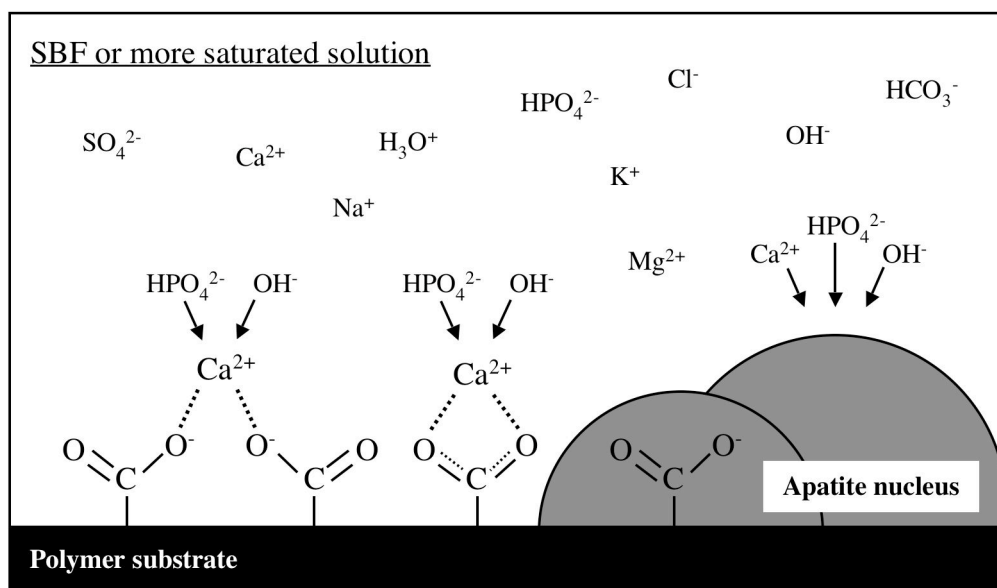


**Figure 3.** Mechanism of hydroxyapatite nucleation.

## *General Introduction*

---

them were aimed at inducing hydroxyapatite nucleation by chemical modifications of the organic polymer to produce nucleation sites. However, the relationship between the arrangement of functional groups and hydroxyapatite formation has not been well considered.

Formation of hydroxyapatite also occurs in the living body to produce bone and teeth. This hydroxyapatite formation, so-called biomineralization, normally relates to many kinds of proteins. For instance, osteocalcin, the most abundant noncollagenous protein in bone, plays an important role in binding to hydroxyapatite because it contains  $\gamma$ -carboxylated glutamic acids (Gla) residues. The domain containing Gla residues in osteocalcin has an  $\alpha$  helix structure, and it provides the precise calcium-binding sites that allow binding to hydroxyapatite with a spatial matching [60]. Dentin matrix protein 1 (DMP1), a protein that is present in bone and teeth, is also thought to play a structural and/or regulatory role during mineral formation: the self-assembled  $\beta$  sheet acidic domains in DMP1 could be an ideal template for apatite nucleation [61]. In both cases, the specific structures of the proteins, such as  $\alpha$  helix and  $\beta$  sheet affect the formation of hydroxyapatite. A similar phenomenon is also seen even in shell nacre that is composed of calcium carbonate and an acidic protein matrix containing aspartic acids. The protein has a  $\beta$  sheet structure and the directed arrangement by the  $\beta$  sheets plays an important role in mineral formation with an orientation [62]. These suggest that, not only the contents of acidic functional groups, but also their arrangement, are considerable factors for effective inducement of heterogeneous nucleation of hydroxyapatite.

On the basis of the phenomena described above, this study is focused on the investigation of hydroxyapatite deposition on polypeptides in a solution mimicking body fluid to clarify the relationship between the secondary structure of polypeptide

and hydroxyapatite formation under biomimetic conditions. Clarification of this issue brings important information to obtain a guideline for the design of organic polymer substrates for preparing a novel hydroxyapatite-organic polymer hybrid as well as to understand the mechanism of biomineralization. In particular, the arrangement of functional groups that are essential for effective inducement of heterogeneous nucleation of hydroxyapatite on organic polymer substrate will be demonstrated.

This study considered which proteins would be appropriate for investigating of hydroxyapatite formation as well as for use as a novel material in the biomedical field. As the protein utilized for the mineralization substrates, silk protein was focused on in this study, because of its unique composition of amino acids and secondary structure. Furthermore, silk has been paid much attention in the field of biomedical materials. For instance, silk fiber has been used as a surgical suture for centuries because of its outstanding mechanical strength and potential biocompatibility. In addition, the many functions of silk proteins, fibroin and sericin, were also investigated: fibroin with chemical modification has antimicrobial properties, anticoagulant properties, and affinity to bone tissue without any reduction in mechanical properties; sericin has a proliferative effect of cell, antioxidant effect, tumor-suppression, etc [63-75]. These indicate that silk protein on which hydroxyapatite is deposited has the potential to be a novel material for medical applications.

For the process of hydroxyapatite formation, the author used the biomimetic aqueous solution, known as 1.5SBF, that has 1.5 times the ion concentrations of SBF. Figure 4 shows logarithms of the degree of supersaturation of hydroxyapatite in the various kinds of biomimetic solutions. The values of the degree of

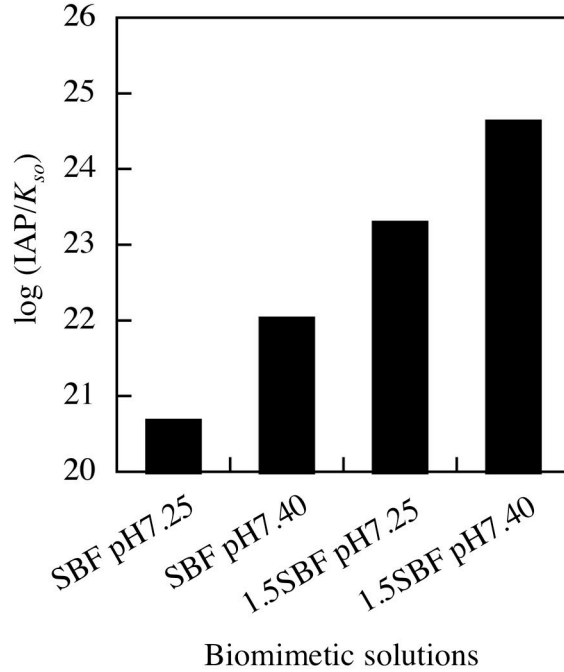


**Figure 4.** Logarithms of the degree of supersaturation of hydroxyapatite in the various kinds of biomimetic solutions.

supersaturation ( $IAP/K_{so}$ ) were calculated from ionic activity products (IAP) with respect to stoichiometric hydroxyapatite given by the following equation,

$$IAP = (\gamma_{Ca^{2+}})^{10} (\gamma_{PO_4^{3-}})^6 (\gamma_{OH^-})^2 \times [Ca^{2+}]^{10} [PO_4^{3-}]^6 [OH^-]^2$$

where  $\gamma$  is the activity coefficient and  $[ ]$  is the concentration of each ion, and the solubility product of hydroxyapatite in an aqueous solution ( $K_{so} = 5.5 \times 10^{-118}$ ) [43]. The degree of supersaturation of hydroxyapatite increases according to the increase in pH and the ion concentrations of the biomimetic solutions. The facility of the heterogeneous nucleation of hydroxyapatite is related to the degree of supersaturation, and a greater degree of supersaturation results in hydroxyapatite



nucleation occurring more rapidly. It should be mentioned that these are able to be metastable solutions, at least for 7 days, even in the case of 1.5SBF.

In Chapter 1, hydroxyapatite formation on the surfaces of silk fibers in 1.5SBF was investigated. Raw silk fiber obtained by filature of cocoon filaments is composed of core fibers of fibroin and surrounding sericin. Degummed silk (normal silk) fiber is obtained by elimination of surface sericin as shown in Figure 5. In other words, different surfaces in terms of their composition of amino acids can be

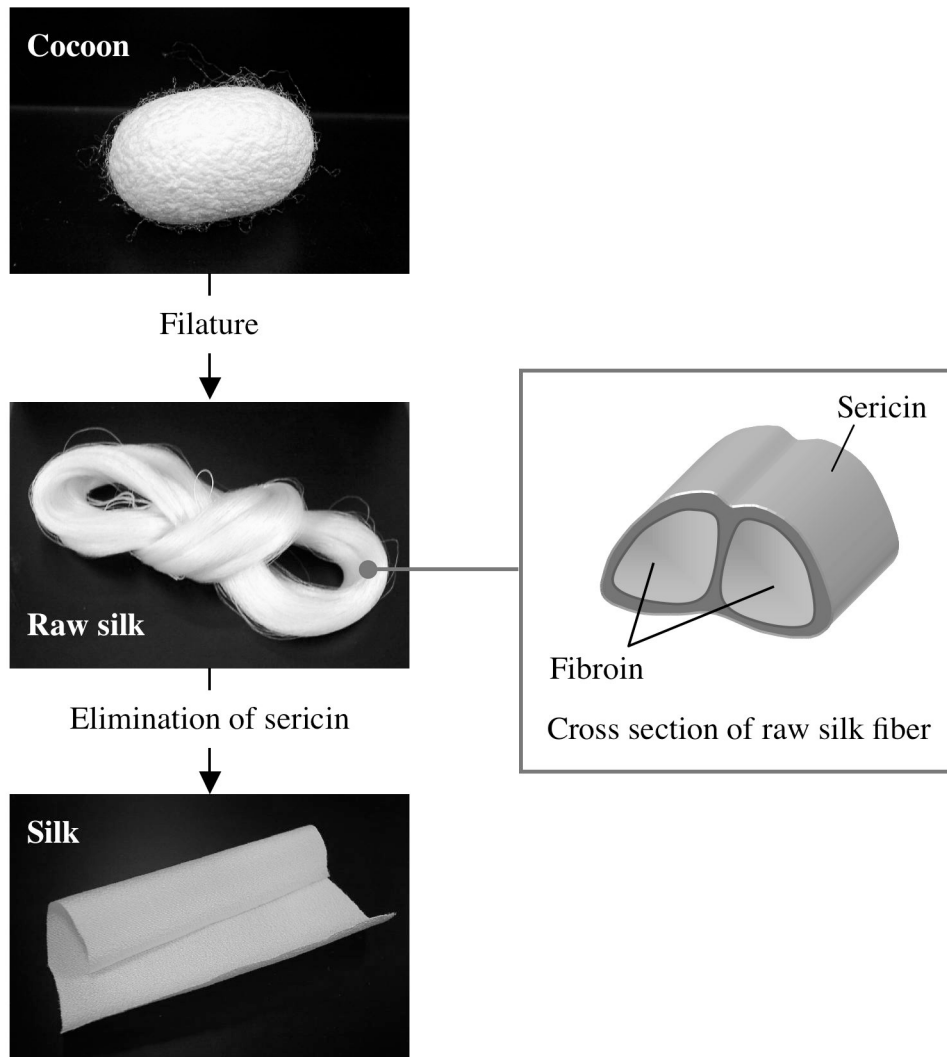


**Figure 5.** Structure of silk fiber.

easily obtained. Therefore, two kinds of fabrics made from raw silk and normal silk were examined. The potential of silk protein as a novel substrate for hydroxyapatite coating was proposed.

In Chapter 2, the structural effect of sericin on hydroxyapatite formation was investigated. Sericin may be a suitable protein for investigating the structural effects on hydroxyapatite-formation because its structure can be easily changed [76-79]. Sericin films with different structures were prepared under various conditions and their hydroxyapatite-forming ability was examined. The results were discussed in terms of secondary structure and molecular weight of sericin.

In Chapter 3, hydroxyapatite deposition on synthetic polypeptide surface was examined to confirm the structural effect of the polypeptides on hydroxyapatite formation. Some polypeptides were designed on the basis of the findings in Chapter 2 and their hydroxyapatite-forming ability was examined.

In the General Summary, the contents of the above chapters were summarized along with the general conclusion of the present thesis and future perspectives.

## **References**

- [1] Rho JY, Kuhn-Spearing L, Zioupos P. Mechanical properties and the hierarchical structure of bone. *Med Eng Phys* 1998;20:92-102.
- [2] Hulbert SF. The use of alumina and zirconia in surgical implants. In: Hench LL, Wilson J, editors. *An Introduction to Bioceramics*. Singapore: World Scientific; 1993. p 25-40.

- [3] Hench LL, Splinger RJ, Allen WC, Greenlee TK. Bonding mechanisms at the interface of ceramic prosthetic materials. *J Biomed Mater Res Symp* 1972;2:117-141.
- [4] Hench LL. Bioceramics; From concept to clinic. *J Am Ceram Soc* 1991;74:1487-1510.
- [5] Hench LL. Bioceramics. *J Am Ceram Soc* 1998;81:1705-1728.
- [6] Jarcho M, Kay JL, Gumaer RH, Drobeck HP. Tissue, cellular and subcellular events at bone-ceramic hydroxyapatite interface. *J Bioeng* 1977;1:79-92.
- [7] LeGeros RZ, LeGeros JP. Dense hydroxyapatite. In: Hench LL, Wilson J, editors. *An Introduction to Bioceramics*. Singapore: World Scientific; 1993. p 139-180.
- [8] Gross UM, Müller-Mai C, Voigt C. Ceravital® bioactive ceramics. In: Hench LL, Wilson J, editors. *An Introduction to Bioceramics*. Singapore: World Scientific; 1993. p 105-124.
- [9] Kokubo T, Shigematsu M, Nagashima Y, Tashiro M, Nakamura T, Yamamuro T, Higashi S. Apatite- and wollastonite-containing glass-ceramics for prosthetic application. *Bull Inst Chem Res, Kyoto Univ* 1982;60:260-268.
- [10] Kokubo T. A/W glass-ceramic: Processing and properties. In: Hench LL, Wilson J, editors. *An Introduction to Bioceramics*. Singapore: World Scientific; 1993. p 75-88.
- [11] Neo M, Nakamura T, Ohtsuki C, Kokubo T, Yamamuro T. Apatite formation on three kinds of bioactive material at an early stage in vivo: a comparative study by transmission electron microscopy. *J Biomed Mater*

- Res 1993;27:999-1006.
- [12] Kokubo T, Kushitani H, Sakka S, Kitsugi T, Yamamuro T. Solutions able to reproduce *in vivo* surface-structure change in bioactive glass-ceramic A-W. J Biomed Mater Res 1990;24:721-734.
- [13] Kokubo T, Miyaji F. Seramikkuseitaizairyō. In: Sato A, Ishikawa T, Sakurai Y, Nakamura A editors. Biocompatibility of biomaterials. Tokyo: Nakayamashoten; 1998. p. 39-46 [in Japanese].
- [14] Kim HM, Miyaji F, Kokubo T, Nakamura T. Preparation of bioactive Ti and its alloys via simple chemical treatment. J Biomed Mater Res 1996;32:409-417.
- [15] Kim HM, Miyaji F, Kokubo T, Nakamura T. Effect of heat treatment on apatite-forming ability of Ti metal induced by heat treatment. J Mater Sci Mater Med 1997;8:341-347.
- [16] Yan WQ, Nakamura T, Kobayashi M, Kim HM, Miyaji F, Kokubo T. Bonding of chemically treated titanium implants to bone. J Biomed Mater Res 1997;37:267-275.
- [17] Yan WQ, Nakamura T, Kawanabe K, Nishiguchi S, Oka M, Kokubo T. Apatite layer-coated titanium for use as bone bonding implants. Biomaterials 1997;18:1185-1190.
- [18] Nishiguchi S, Nakamura T, Kobayashi M, Kim HM, Miyaji F, Kokubo T. The effect of heat treatment on bone-bonding ability of alkali-treated titanium. Biomaterials 1999;20:491-500.
- [19] Nishiguchi S, Kato H, Fujita H, Kim HM, Miyaji F, Kokubo T, Nakamura T. Enhancement of bone-bonding strength of titanium alloy implants by alkali

- and heat treatments. *J Biomed Mater Res* 1999;48:689-696.
- [20] Miyazaki T, Kim HM, Miyaji F, Kokubo T, Kato H, Nakamura T. Bioactive tantalum metal prepared by NaOH treatment. *J Biomed Mater Res* 2000;50:35-42.
- [21] Kato H, Nakamura T, Nishiguchi S, Matsusue Y, Kobayashi M, Miyazaki T, Miyaji F, Kim HM, Kokubo T. Bonding of alkali- and heat-treated tantalum implants to bone. *J Biomed Mater Res: Appl Biomater* 2000;53:28-35.
- [22] Miyazaki T, Kim HM, Kokubo T, Miyaji F, Kato H, Nakamura T. Effect of thermal treatment on apatite-forming ability of NaOH-treated tantalum metal. *J Mater Sci Mater Med* 2001;12:683-687.
- [23] Ohtsuki C, Iida H, Hayakawa S, Osaka A. Bioactivity of titanium treated with hydrogen peroxide solutions containing metal chlorides. *J Biomed Mater Res* 1998;35:39-47.
- [24] Weiner S, Wagner HD. The material bone: structure mechanical function relations. *Annu Rev Mater Sci* 1998;28:271-298.
- [25] Robinson RA. An electron-microscopic study of the crystalline inorganic component of bone and its relationship to the organic matrix. *J Bone Joint Surg A* 1952;34:389-476.
- [26] Park JB, Lakes RS. In: *Biomaterials* 2nd Ed. New York: Plenum Press; 1992. p 185-222.
- [27] Bonfield W, Grynblas MD, Tully AE. Hydroxyapatite reinforced polyethylene – a mechanically compatible implant material for bone replacement. *Biomaterials* 1981;2:185-186.
- [28] Bonfield W. Design of bioactive ceramic-polymer composites. In: Hench LL,

- Wilson J, editors. An Introduction to bioceramics. Singapore: World Scientific; 1993. p 299-303.
- [29] Rey C. Calcium phosphate biomaterials and bone mineral. Differences in composition, structures and properties. *Biomaterials* 1990;11:13-15.
- [30] Neuman W, Neuman M. In: The chemical dynamics of bone mineral. Chicago: The University of Chicago Press; 1958. p 1-38.
- [31] Abe Y, Kokubo T, Yamamuro T. Apatite coating on ceramics, metals and polymers utilizing a biological process. *J Mater Sci Mater Med* 1990;1:233-238.
- [32] Tanahashi M, Yao T, Kokubo T, Minoda M, Miyamoto T, Nakamura T, Yamamuro T. Apatite coating on organic polymers by a biomimetic process. *J Am Ceram Soc* 1994;77:2805-2808.
- [33] Miyaji F, Kim HM, Handa S, Kokubo T, Nakamura T. Bonelike apatite coating on organic polymers: novel nucleation process using sodium silicate solution. *Biomaterials* 1999;20:913-919.
- [34] Kim HM, Uenoyama M, Kokubo T, Minoda M, Miyamoto T, Nakamura T. Biomimetic apatite formation on polyethylene photografted with vinyltrimethoxysilane and hydrolyzed. *Biomaterials* 2001;22:2489-2494.
- [35] Taguchi T, Muraoka Y, Matsuyama H, Kishida A, Akashi M. Apatite coating on hydrophilic polymer-grafted poly(ethylene) films using an alternate soaking process. *Biomaterials* 2001;22:53-58.
- [36] Rhee SH, Tanaka J. Effect of citric acid on the nucleation of hydroxyapatite in a simulated body fluid. *Biomaterials* 1999;20:2155-2160.
- [37] Li F, Feng QL, Cui FZ, Li HD, Schubert H. A simple biomimetic method for

- calcium phosphate coating. *Surf Coat Technol* 2001;154:88-89.
- [38] Habibovic P, Barrere F, van Blitterswijk CA, de Groot K, Layrolle P. Biomimetic coating on metal implants. *J Am Ceram Soc* 2002;85:517-522.
- [39] Hata K, Kokubo T, Nakamura T, Yamamuro T. Growth of a bonelike apatite layer on a substrate by a biomimetic process. *J Am Ceram Soc* 1995;78:1049-1053.
- [40] Takadama H, Kim HM, Kokubo T, Nakamura T. Mechanism of apatite formation induced by silanol groups: TEM observation. *J Ceram Soc Japan* 2000;108:118-121.
- [41] Tanahashi M, Kokubo T, Nakamura T, Katsura Y, Nagano M. Ultrastructural study of an apatite layer formed by a biomimetic process and its bonding to bone. *Biomaterials* 1996;17:47-51.
- [42] Ohtsuki C, Kokubo T, Takatsuka K, Yamamuro T. Compositional dependence of bioactivity of glasses in the system CaO-SiO<sub>2</sub>-P<sub>2</sub>O<sub>5</sub>: Its *in vitro* evaluation. *J Ceram Soc Japan* 1991;99:1-6.
- [43] Ohtsuki C, Kokubo T, Yamamuro T. Mechanism of apatite formation on CaO-SiO<sub>2</sub>-P<sub>2</sub>O<sub>5</sub> glasses in a simulated body fluid. *J Non-Cryst Solids* 1992;143:84-92.
- [44] Li P, Ohtsuki C, Kokubo T, Nakanishi K, Soga N, Nakamura T, Yamamuro T. Apatite formation induced by silica gel in a simulated body fluid. *J Am Ceram Soc* 1992;75:2094-2097.
- [45] Li P, Ohtsuki C, Kokubo T, Nakanishi K, Soga N, Nakamura T, Yamamuro T. Effects of ion in aqueous media on hydroxyapatite induction by silica gel and its relevance to bioactivity of bioactive glasses and glass-ceramics. *J*

- Appl Biomater 1993;4:221-229.
- [46] Li P, Ohtsuki C, Kokubo T, Nakanishi K, Soga N, de Groot K. The role of hydrated silica, titania and alumina in inducing apatite on implants. *J Biomed Mater Res* 1994;28:7-15.
- [47] Takadama H, Kim HM, Kokubo T, Nakamura T. An X-ray photoelectron spectroscopic study of the process of apatite formation on bioactive titanium metal. *J Biomed Mater Res* 2001;55:185-193.
- [48] Uchida M, Kim HM, Kokubo T, Fujibayashi S, Nakamura T. Structural dependence of apatite formation on titania gel in a simulated body fluid. *J Biomed Mater Res* 2003;64A:164-170.
- [49] Uchida M, Kim HM, Miyaji F, Kokubo T, Nakamura T. Bonelike apatite formation induced on zirconia gel in a simulated body fluid and its modified solutions. *J Am Ceram Soc* 2001;84:2041-2044.
- [50] Miyazaki T, Kim HM, Kokubo T, Kato H, Nakamura T. Induction and acceleration of bonelike apatite formation on tantalum oxide gel in simulated body fluid. *J Sol-gel Sci Tech* 2001;21:83-88.
- [51] Miyazaki T, Kim HM, Kokubo T, Ohtsuki C, Nakamura T. Apatite-forming ability of niobium oxide gels in a simulated body fluid. *J Ceram Soc Japan* 2001;109:929-933.
- [52] Tanahashi M, Matsuda T. Surface functional group dependence on apatite formation on self-assembled monolayers in a simulated body fluid. *J Biomed Mater Res* 1997;34:305-315.
- [53] Kawai T, Ohtsuki C, Kamitakahara M, Miyazaki T, Tanihara M, Sakaguchi Y, Konagaya S. Coating of an apatite layer on polyamide films containing



- sulfonic groups by a biomimetic process. *Biomaterials* 2004;25:4529-4534.
- [54] Miyazaki T, Ohtsuki C, Akioka Y, Tanihara M, Nakao J, Sakaguchi Y, Konagaya S. Apatite deposition on polyamide film containing carboxyl group in a biomimetic solution. *J Mater Sci Mater Med* 2003;14:569-574.
- [55] Hosoya K, Ohtsuki C, Kawai T, Kamitakahara M, Ogata S, Miyazaki T, Tanihara M. A novel covalently crosslinked gel of alginate and silane with the ability to form bone-like apatite.
- [56] Kim HM, Uenoyama M, Kokubo T, Minoda M, Miyamoto T, Nakamura T. Biomimetic apatite formation on polyethylene photografted with vinyltrimetoxysilane and hydrolyzed. *Biomaterials* 2001;22:2489-2494.
- [57] Kawashita M, Nakao M, Minoda M, Kim HM, Beppu T, Miyamoto T, Kokubo T, Nakamura T. Apatite-forming ability of carboxyl group containing polymer gels in a simulated body fluid. *Biomaterials* 2003;24:2477-2484.
- [58] Kokubo T, Hanakawa M, Kawashita M, Minoda M, Beppu T, Miyamoto T, Nakamura T. Apatite-forming ability of alginate fibers treated with calcium hydroxide solution. *J Mater Sci Mater Med* 2004;15:1007-1012.
- [59] Kokubo T, Hanakawa M, Kawashita M, Minoda M, Beppu T, Miyamoto T, Nakamura T. Apatite-formation on non-woven fabric of carboxymethylated chitin in SBF. *Biomaterials* 2004;25:4485-4488.
- [60] Hoang QQ, Sichert F, Haward AJ, Yang DSC. Bone recognition mechanism of porcine osteocalcin from crystal structure. *Nature* 2003;425:977-980.
- [61] He G, Dahl T, Veis A, Eorge A. Nucleation of apatite crystals *in vitro* by self-assembled dentin matrix protein 1. *Nature Materials* 2003;2:552-558.
- [62] Addadi L, Weiner S. Interactions between acidic proteins and crystals:

- Stereochemical requirements in biomineralization. *Proc Natl Acad Sci USA* 1985;82:4110-4114.
- [63] Furuzono T, Ishihara K, Nakabayashi N, Tamada Y. Chemical modification of silk fibroin with 2-methacryloxyethyl phosphorylcholine. II. Graft-polymerization onto fabric through 2-methacryloxyethyl isocyanate and interaction between fabric and platelets. *Biomaterials* 2000;21:327-333.
- [64] Furuzono T, Taguchi T, Kishida A, Akashi M, Tamada Y. Preparation and characterization of apatite deposited on silk fabric using an alternate soaking process. *J Biomed Mater Res* 2000;50:344-352.
- [65] Altman GH, Daiz F, Jakuba C, Calabro T, Horan RL, Chen J, Lu H, Richmond J, Kaplan DL. Silk-based biomaterials. *Biomaterials* 2003;24:401-416.
- [66] Furuzono T, Kishida A, Tanaka J. Nano-scaled hydroxyapatite/polymer composite I. Coating of sintered hydroxyapatite particles on poly( $\gamma$ -methacryloxypropyl trimethoxysilane)-grafted silk fibroin fibers through chemical bonding. *J Mater Sci Mater Med* 2004;15:19-23.
- [67] Furuzono T, Yasuda S, Kimura T, Kyotani S, Tanaka J, Kishida A. Nano-scaled hydroxyapatite/polymer composite IV. Fabrication and cell adhesion properties of a three-dimensional scaffold made of composite material with silk fibroin substrate to develop a percutaneous device. *J Artif Organs* 2004;7:137-144.
- [68] Tamada Y. Addition of new functions to silk proteins by chemical modification and their applications. *Bio Industry* 2004;21:54-60 [in Japanese].

- [69] Tsujimoto K, Takagi H, Takahashi M, Yamada H, Nakamori S. Cryoprotective effect of the serine-rich repetitive sequence in silk protein sericin. *J Biochem* 2001;129:979-986.
- [70] Zhang YQ. Applications of natural silk protein sericin in biomaterials. *Biotechnology Advances* 2002;20:91-100.
- [71] Terada S, Nishimura T, Sasaki M, Yamada H, Miki M. Sericin, a protein derived from silkworms, accelerates the proliferation of several mammalian cell lines including a hybridoma. *Cytotechnology* 2002;40:3-12.
- [72] Takahashi M, Tsujimoto K, Yamada H, Takagi H, Nakamori S. The silk protein, sericin protects against cell death caused by acute serum deprivation in insect cell culture. *Biotech Lett* 2003;25:1805-1809.
- [73] Tsujimoto K. Development of the functional fabric using the silk protein. *Bio Industry* 2004;21:46-53 [in Japanese].
- [74] Sasaki M, Kato Y, Yamada H, Terada S. Development of a novel serum-free freezing medium for mammalian cells using the silk protein sericin. *Biotechnol Appl Biochem* 2005;42:183-188.
- [75] Zhang YQ. Applications of natural silk protein sericin in biomaterials. *Biotechnology Advances* 2002;20:91-100.
- [76] Komatsu K. Chemical and structural characteristics of silk sericin. In: Hojo N, editor. *Structure of silk yarn, Part B: Chemical structure and processing of silk yarn*. Science Publishers, Inc: Enfield (NH); 2000. p. 47-85.
- [77] Takasu Y, Yamada H, Tsubouchi K. Isolation of three main sericin components from the cocoon of the silkworm, *Bombyx mori*. *Biosci Biotechnol Biochem* 2002;66:2715-2718.

- [78] Lee KG, Kweon HY, Yeo JH, Woo SO, Lee YW, Cho CS, Kim KH, Park YH. Effect of methyl alcohol on the morphology and conformational characteristics of silk sericin. *Int J Biol Macromol* 2003;33:75-80.
- [79] Tsujimoto K. Development of the functional fabric using the silk protein. *Bio Industry* 2004;21:46-53 [in Japanese].

# **Chapter 1**

## **Formation of Hydroxyapatite on Silk Fiber in a Solution Mimicking Body Fluid**

### **1. Introduction**

Hydroxyapatite-organic polymer hybrid is expected as a useful material for biomedical application because it shows both high biocompatibility of hydroxyapatite and flexibility of organic polymer. To fabricate such a hybrid, Kokubo *et al.* [1,2] have proposed a coating method of hydroxyapatite called as biomimetic process. In this process, a hydroxyapatite layer was coated on the surface of an organic polymer substrate in a simulated body fluid (SBF) that is an aqueous solution with inorganic ion concentrations nearly equal to human blood plasma (Table 1.1). When a rapid deposition of hydroxyapatite was required, more saturated solutions such as 1.5SBF, which has 1.5 times higher ion concentrations than those of SBF, has been used. Tanahashi *et al.* [3] reported that nucleation of hydroxyapatite in these aqueous solutions induced by specific functional groups on the organic polymer surface, such as carboxyl (-COOH) groups and phosphate (-PO<sub>4</sub>H<sub>2</sub>) groups because they are negatively charged and can interact with Ca<sup>2+</sup> ions

**Table 1.1.** Ion concentrations of simulated body fluid (SBF), 1.5SBF and human plasma

Ion	Concentration / mM		
	Human plasma	SBF	1.5SBF
Na <sup>+</sup>	142.0	142.0	213.0
K <sup>+</sup>	5.0	5.0	7.5
Mg <sup>2+</sup>	1.5	1.5	2.3
Ca <sup>2+</sup>	2.5	2.5	3.8
Cl <sup>-</sup>	103.0	147.8	221.7
HCO <sub>3</sub> <sup>-</sup>	27.0	4.2	6.3
HPO <sub>4</sub> <sup>2-</sup>	1.0	1.0	1.5
SO <sub>4</sub> <sup>2-</sup>	0.5	0.5	0.8

in SBF. Once hydroxyapatite nuclei are formed on the surface of a substrate, they spontaneously grow into a hydroxyapatite layer because SBF is supersaturated with respect to hydroxyapatite even under normal conditions. Therefore, it is a key engineering to find substrates that effectively induce hydroxyapatite nucleation to achieve a successful coating of hydroxyapatite utilizing SBF.

It was previously reported that synthetic polyamide films containing carboxyl groups or sulfonic groups could induce a hydroxyapatite nucleation in 1.5SBF when the films were modified with calcium salts [4,5]. These findings show that organic polymers with specific functional groups can induce heterogeneous nucleation of hydroxyapatite. This study focused on natural polypeptides, silk proteins, as organic substrates for coating of hydroxyapatite. Because silk fiber is a

natural organic fiber derived from silkworm that has a possibility of being used as biomaterials owing to their biological properties. For instance, proteins consisting of silk fiber, fibroin and sericin, have been studied in the field of biomaterials science in recent years, and their excellent functions such as the ability to accelerate cell proliferation were documented [6-17].

The structures of silk fibers are shown in Figure 1.1. Raw silk fiber is obtained by filature of silkworm cocoon filament. This is composed of core fibers of fibroin and surrounding sericin. Degummed silk (normal silk) fiber is obtained by elimination of surface sericin from raw silk fiber. In other words, these fibers contain different kinds of proteins, fibroin and sericin, on their surfaces respectively. Two kinds of woven fabrics made from raw silk and normal silk were first soaked in 1.5SBF to examine hydroxyapatite formation on the silk proteins.

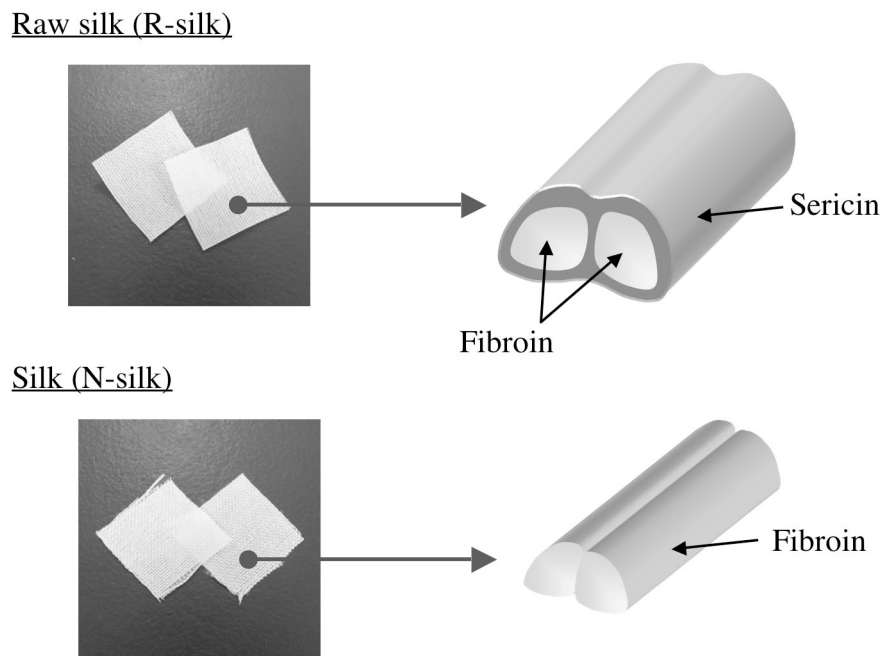


**Figure 1.1.** Macroscopic images of the samples examined in this study.

## **2. Experimental procedure**

### **2.1. Preparation of specimens**

Two types of silk fabrics were supplied from the Kyoto Prefectural Institute for Northern Industry, Japan: one was made from raw silk fiber, and the second from degummed silk (normal silk) fiber. The former was denoted as R-silk, and the latter was as N-silk in this study. Macroscopic images of these fabrics were shown in Figure 1.1. Specimens were cut from the fabrics into a sheet of dimensions 10 mm×10 mm, and washed with ultra-pure water. The film made from sericin solution was also prepared. An aqueous solution containing 0.3 mass% of sericin, supplied from the Kyoto Prefectural Institute for Northern Industry, Japan, was dropped into a polystyrene Petri dish, and it was allowed to dry at room temperature in air to form a sericin film at the bottom of the dish.

### **2.2. CaCl<sub>2</sub> treatment of the specimens**

Aqueous solutions containing CaCl<sub>2</sub> (Nacalai Tesque Inc., Japan) in concentration of 0.01, 0.1, 1 or 5 M (=kmol·m<sup>-3</sup>) were prepared. The samples of R-silk and N-silk were soaked in 30 mL of the CaCl<sub>2</sub> aqueous solutions in various concentrations at 36.5°C respectively. After keeping at 36.5°C for 24 hours, the samples were rinsed with ultra-pure water.

### **2.3. Soaking in 1.5SBF**

The specimens of R-silk and N-silk, with and without the CaCl<sub>2</sub> treatment, were soaked in 30 mL of 1.5SBF at 36.5°C. After keeping at 36.5°C for 7 days, they were rinsed with ultra-pure water and dried at room temperature in air. The sericin film formed at the bottom of Petri dish was also exposed to 15 mL of 1.5SBF at



36.5°C for 7 days, rinsed with ultra-pure water, and dried. The solution, 1.5SBF, was prepared using the method reported by Kokubo *et al.* [2]. The amounts of chemicals using for preparing 1 liter (=L) of 1.5SBF were summarized in Table 1.2. The chemicals of NaCl, NaHCO<sub>3</sub>, KCl, K<sub>2</sub>HPO<sub>4</sub>·3H<sub>2</sub>O, MgCl<sub>2</sub>·6H<sub>2</sub>O, CaCl<sub>2</sub>, and Na<sub>2</sub>SO<sub>4</sub> (Nacalai Tesque Inc., Japan) were dissolved in 700 mL of ultra-pure water, one by one in the order given on Table 1.2, at 36.5°C. The pH of the solution was buffered at 7.25 using 75 mol·m<sup>-3</sup> of tris(hydroxymethyl)aminomethane (Nacalai Tesque Inc., Japan) along with an appropriate volume of 1 kmol·m<sup>-3</sup> hydrochloric acid solution. After cooling at room temperature, the total volume of the solution was adjusted to 1 L using measuring flask by adding ultra-pure water.

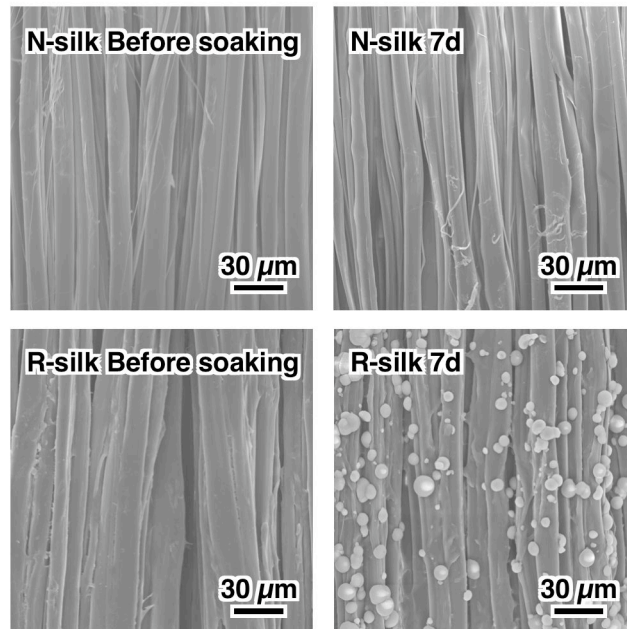
**Table 1.2.** Chemicals used for preparation of 1.5SBF

Order	Reagent	Amount
1	NaCl	11.994 g
2	NaHCO <sub>3</sub>	0.525 g
3	KCl	0.336 g
4	K <sub>2</sub> HPO <sub>4</sub> ·3H <sub>2</sub> O	0.342 g
5	MgCl <sub>2</sub> ·6H <sub>2</sub> O	0.458 g
6	1 kmol·m <sup>-3</sup> HCl	60 mL
7	CaCl <sub>2</sub>	0.417 g
8	Na <sub>2</sub> SO <sub>4</sub>	0.107 g
9	NH <sub>2</sub> C(CH <sub>2</sub> OH) <sub>3</sub>	9.086 g

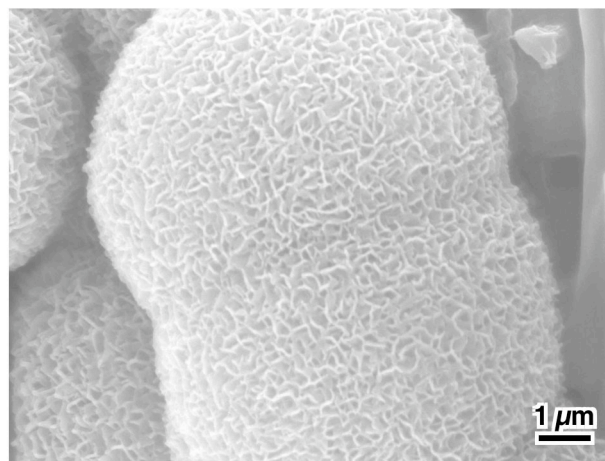
The surfaces of the specimens both before and after soaking in 1.5SBF were observed under a scanning electron microscope (SEM; S-3500N, Hitachi Co., Ltd., Tokyo, Japan) equipped with an energy dispersive X-ray microanalyser (EDX; EMAX ENERGY EX-400, HORIBA, Ltd., Kyoto, Japan). The surfaces of the fibers were also characterized using X-ray fluorescence element analysis (XRF, MESA-500, Horiba, Ltd., Japan) employing a rhodium target and thin-film X-ray diffraction (TF-XRD; M18XHF<sup>22</sup>-SRA, MAC Science Co., Ltd., Yokohama, Japan). In the SEM observations, the surfaces of some of the specimens were coated with sputtered gold. In the TF-XRD apparatus, the incident beam was set at 1° against the specimen.

### 3. Results

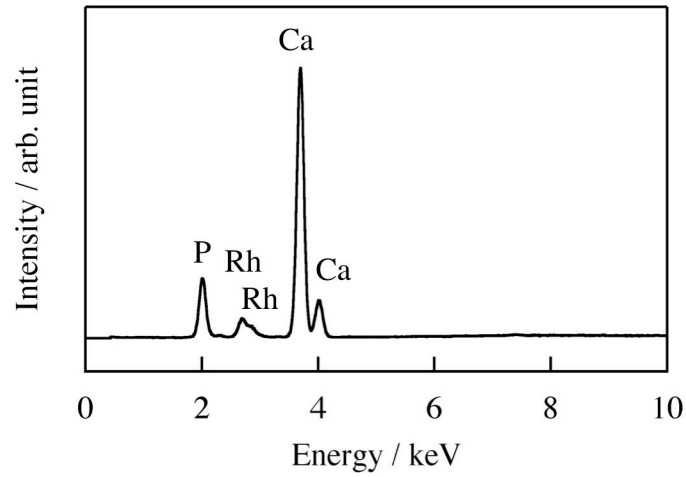
Figure 1.2 shows SEM images of R-silk and N-silk surfaces without any CaCl<sub>2</sub> treatments, before and after soaking in 1.5SBF at 36.5°C for 7 days. Any changes were not observed between N-silk surfaces before and after soaking in 1.5SBF. On the other hand, spherical particles with 2-3 μm in diameter were observed on R-silk surface soaked in 1.5SBF. Figure 1.3 shows SEM image of the deposited particles on the R-silk surface after soaking in 1.5SBF for 7 days. The morphology of these particles was that of an assembly consisting of finer particles. This morphology is similar to that of hydroxyapatite crystals observed on bioactive glasses soaked in SBF [18,19]. Figure 1.4 shows XRF spectrum of these particles on the R-silk surface. This result indicates that particles predominantly contained calcium and phosphorus. These results indicate that small quantities of hydroxyapatite are deposited on the surface of R-silk after exposure to 1.5SBF.



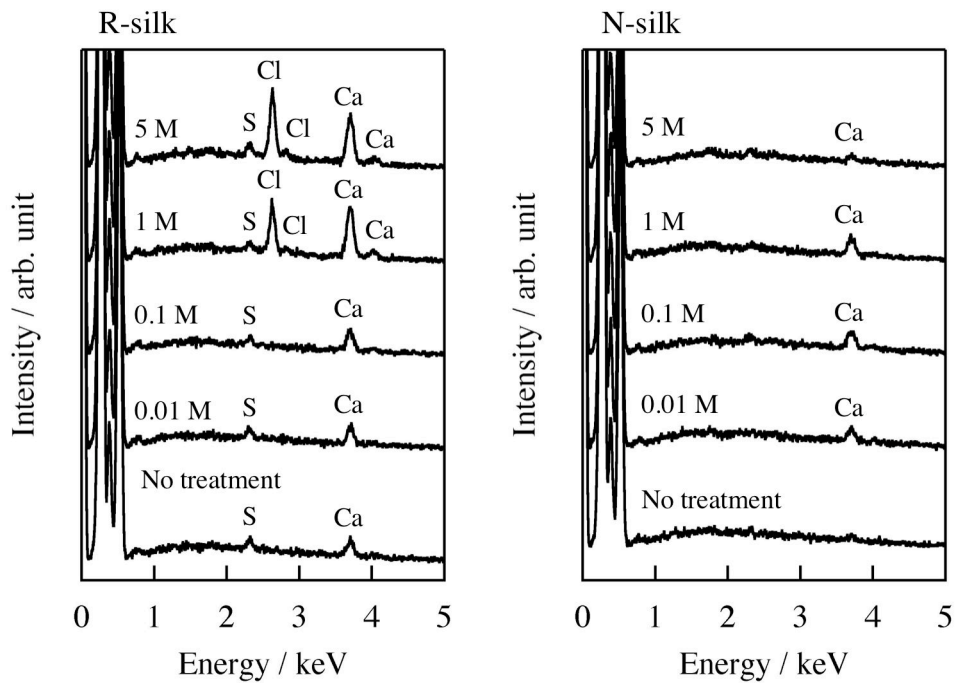
**Figure 1.2.** SEM images of the surfaces of N-silk and R-silk before and after soaking in 1.5SBF for 7 days.



**Figure 1.3.** SEM image of the deposited particles on the surface of R-silk after soaking in 1.5SBF for 7 days.

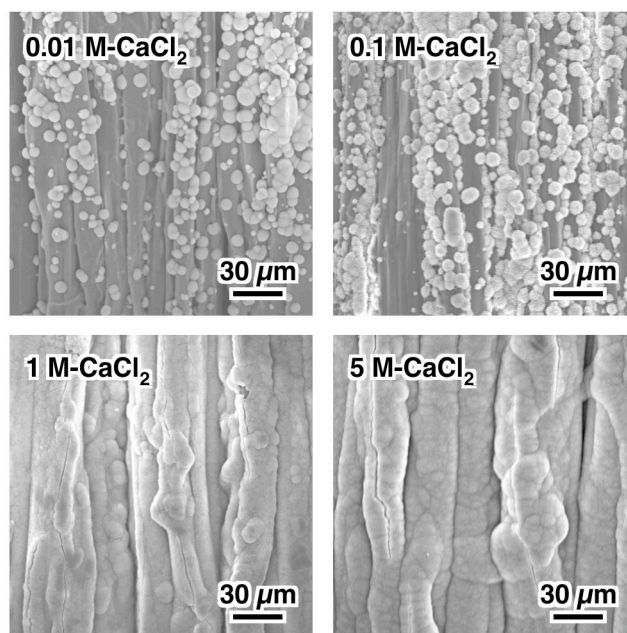


**Figure 1.4.** XRF spectrum of the deposited particles on the surface of R-silk after soaking in 1.5SBF for 7 days.

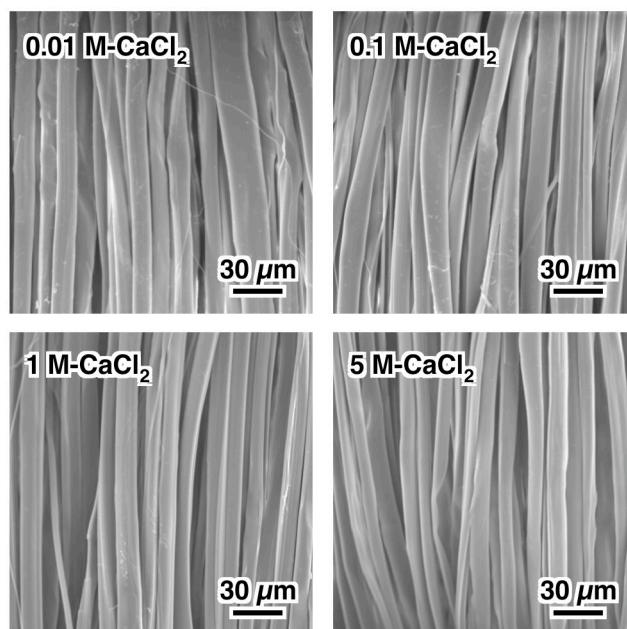


**Figure 1.5.** EDX spectra of the surfaces of R-silk and N-silk before and after treatment with various concentrations of  $\text{CaCl}_2$  solution. ( $M = \text{kmol} \cdot \text{m}^{-3}$ )

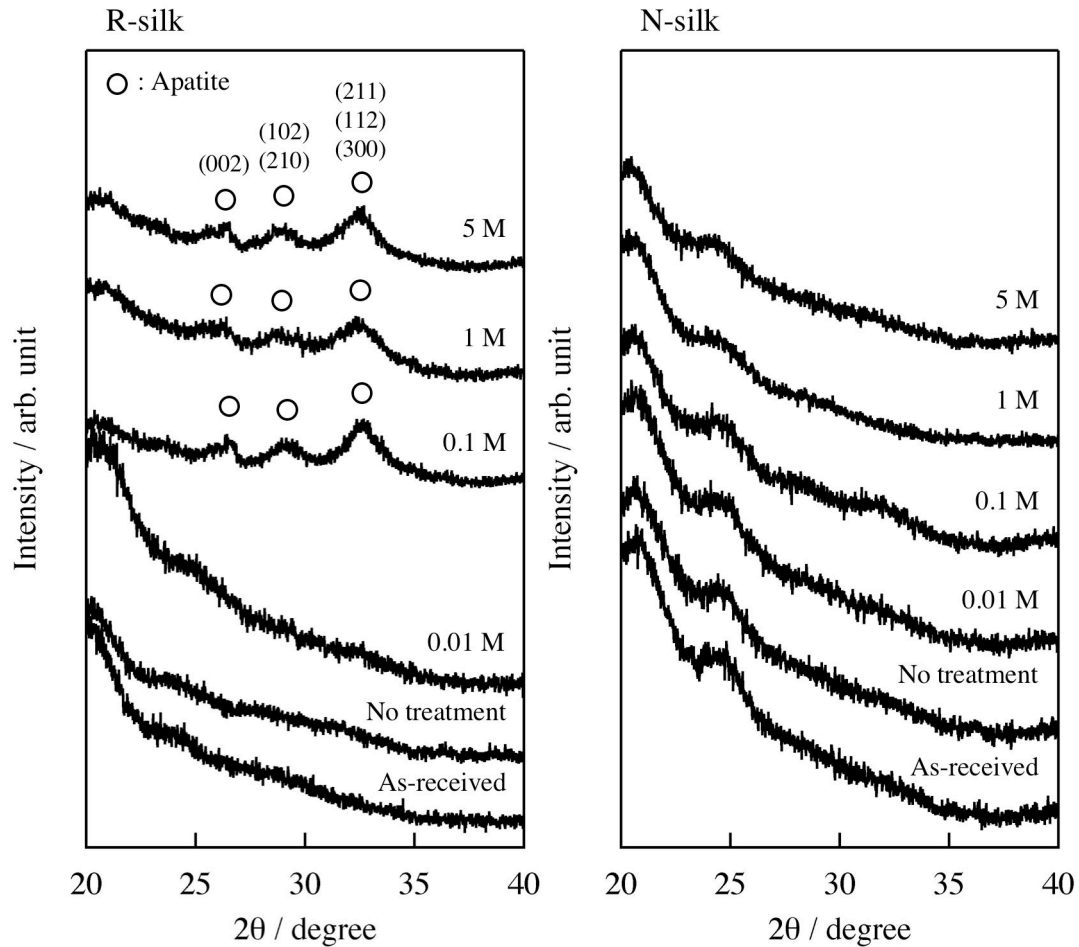
In SEM observations on R-silk and N-silk surfaces before and after treatment with various concentrations of  $\text{CaCl}_2$  aqueous solutions, any changes were not observed on the surfaces of specimens. Figure 1.5 shows EDX spectra of R-silk and N-silk surfaces before and after treatment with  $\text{CaCl}_2$  aqueous solutions. A peak assigned to calcium detected for R-silk without the  $\text{CaCl}_2$  treatment was attributed to calcium contained in sericin naturally. Peak intensity of calcium and chlorine increased according to the increase in concentrations of  $\text{CaCl}_2$  aqueous solutions for R-silk. However, these intensities were not so changed for N-silk even after the  $\text{CaCl}_2$  treatment. Figures 1.6 and 1.7 show SEM images of R-silk and N-silk surfaces that were treated with various concentrations of  $\text{CaCl}_2$  aqueous solutions and subsequently soaked in 1.5SBF for 7 days. It was obvious that the deposition of the fine particles on the R-silk surface had significantly increased to cover whole surface of the fibers after their immersion in 1.5SBF, when the cloth was subjected to a prior treatment with a  $\text{CaCl}_2$  solution at concentrations above 1 M. In contrast, no deposition was observed on the N-silk surface, even when the specimen was treated with  $\text{CaCl}_2$  solutions at concentrations up to 5 M. Figure 1.8 shows TF-XRD patterns of the surface of the specimens treated with various  $\text{CaCl}_2$  concentrations and subsequently soaked in 1.5SBF for 7 days. Broad peaks that could be assigned to hydroxyapatite were detected around  $2\theta = 26$  and  $32^\circ$  for the R-silk treated with  $\text{CaCl}_2$  solutions at concentrations above 0.1 M. These results indicate that particles deposited on R-silk surface were hydroxyapatite and their deposition was accelerated by prior treatment with a solution containing 1 M of  $\text{CaCl}_2$  or more.



**Figure 1.6.** SEM images of the surfaces of R-silk treated with various concentrations of CaCl<sub>2</sub> solution, followed by soaking in 1.5SBF for 7 days. (M=kmol·m<sup>-3</sup>)



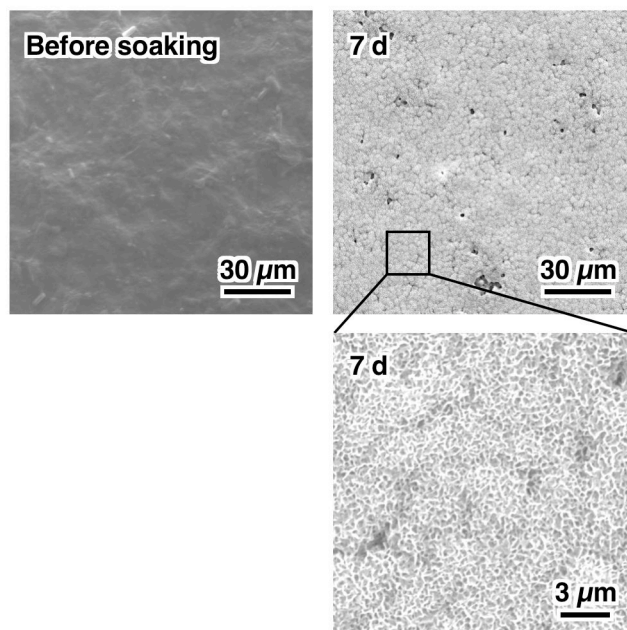
**Figure 1.7.** SEM images of the surfaces of N-silk treated with various concentrations of CaCl<sub>2</sub> solution, followed by soaking in 1.5SBF for 7 days. (M=kmol·m<sup>-3</sup>)



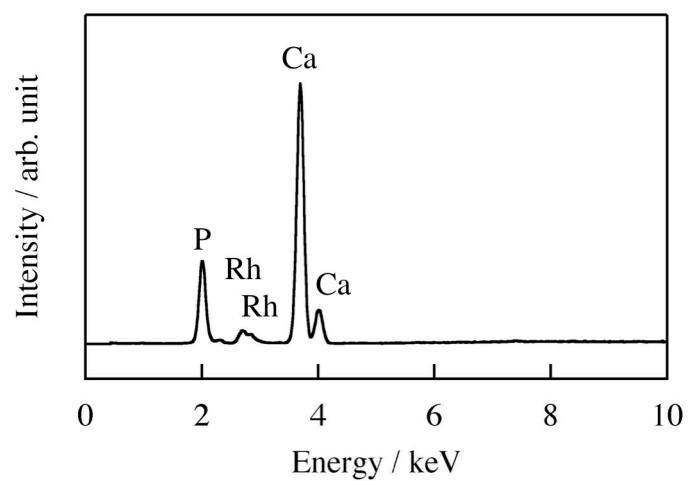
**Figure 1.8.** TF-XRD patterns of the surfaces of R-silk and N-silk treated with various concentrations of  $\text{CaCl}_2$  solution, followed by soaking in 1.5SBF for 7 days. ( $M = \text{kmol} \cdot \text{m}^{-3}$ )

Figure 1.9 shows SEM images of sericin film surfaces before and after soaking in 1.5SBF for 7 days. Assemblies of fine particles with similar morphologies to those seen in R-silk surface soaked in 1.5SBF were observed on sericin film surface after soaking in 1.5SBF. The result of XRF analysis of sericin films after soaking in 1.5SBF is shown in Fig. 1.10. It is obvious from the XRF spectrum that calcium and phosphorus are the dominant inorganic constituents of the sericin film after soaking in 1.5SBF for 7 days. This result supports the proposition that the deposited particles consist of hydroxyapatite.





**Figure 1.9.** SEM images of the surfaces of sericin films before and after soaking in 1.5SBF for 7 days. (Below image: at higher magnification)



**Figure 1.10.** XRF spectrum of the surface of sericin film after soaking in 1.5SBF for 7 days.



#### **4. Discussion**

It is apparent from the results seen in Figure 1.2, that R-silk has the ability to deposit hydroxyapatite in 1.5SBF, although the rate of hydroxyapatite deposition is not enough to cover the entire surface of the fibers within 7 days. In contrast, N-silk does not have the ability to deposit hydroxyapatite under the same conditions. This indicates that the surface of the R-silk has the potential to induce heterogeneous nucleation of hydroxyapatite in 1.5SBF. Hydroxyapatite deposition is known to be initiated by some functional groups that exist on the surface of a material [20,21]. Therefore, the R-silk must have specific functional sites for hydroxyapatite nucleation on its surface. R-silk consists of sericin and N-silk consists of fibroin, as shown in Figure 1.1. Namely, the heterogeneous deposition of hydroxyapatite on the surface of R-silk is attributed to the presence of sericin. The ability of sericin to form hydroxyapatite is confirmed by the results seen in Figures. 1.9 and 1.10. Consequently, it was clarified that sericin has the ability to induce heterogeneous nucleation of hydroxyapatite in 1.5SBF.

The potential of sericin to provide heterogeneous nucleation sites for hydroxyapatite is much higher than that of fibroin. Sericin is a protein characterized by about 30 mol% of serine that has hydroxyl (-OH) group in the side chain as given on Table 1.3 [22,23]. Sericin also contains high content of hydrophilic and acidic amino acid as well as serine, threonine and tyrosine with hydroxyl group and aspartic acid and glutamic acid with carboxyl group, and they lead high hydrophilicity surface of sericin. The surface composed of these amino acids of sericin may provide nucleation sites for hydroxyapatite.

Tanahashi *et al.* [3] previously investigated the dependence of surface functional group on hydroxyapatite deposition using self-assembled monolayers

(SAMs) of alkanethiols having methyl (-CH<sub>3</sub>), phosphate (-PO<sub>4</sub>H<sub>2</sub>), carboxyl (-COOH), amide (-CONH<sub>2</sub>), hydroxyl (-OH) and amino (-NH<sub>2</sub>) terminal groups. In their study, the growth rate of hydroxyapatite on the SAMs decreased in the order,

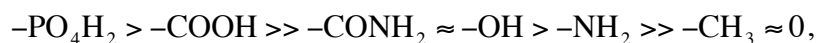
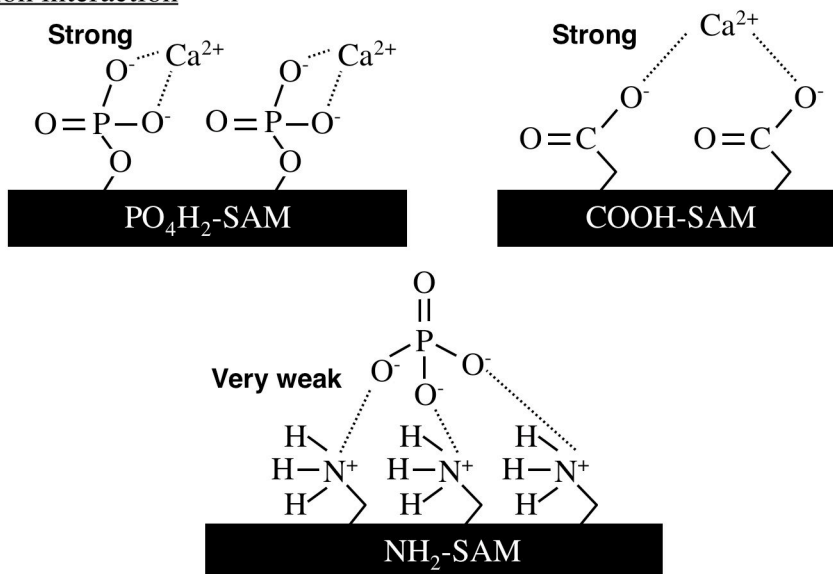


**Table 1.3.** Amino acid compositions of sericin and fibroin (mol%) [22,23]

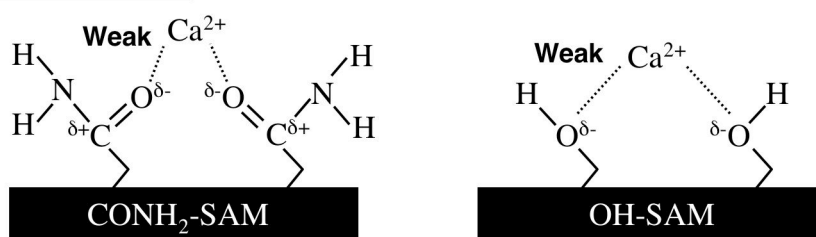
<b>Amino acid</b>	<b>Sericin</b>	<b>Fibroin</b>
Serine	31.97	12.2
Aspartic acid	13.84	1.9
Glycine	12.70	42.9
Threonine	8.25	0.9
Glutamic acid	5.80	1.4
Alanine	5.51	30.0
Tyrosine	3.40	4.8
Lysine	3.26	0.4
Arginine	2.85	0.5
Valine	2.68	2.5
Histidine	1.30	0.2
Leucine	0.72	0.6
Proline	0.57	0.5
Isoleucine	0.55	0.6
Phenylalanine	0.43	0.7
Cysteine	0.14	0.03
Methionine	0.05	0.1

and the rate on  $\text{PO}_4\text{H}_2^-$ - and  $\text{COOH-SAMs}$  after soaking in SBF for 10 days were much higher than that on  $\text{CONH}_2^-$ - and  $\text{OH-SAMs}$ . Specifically, the rate on  $\text{PO}_4\text{H}_2^-$ - and  $\text{COOH-SAMs}$  were  $0.4$  and  $2.4 \times 10^{-3} \mu\text{m/day}$  while  $\text{CONH}_2^-$ - and  $\text{OH-SAMs}$  were  $4 \times 10^{-4}$  and less than  $1 \times 10^{-4} \mu\text{m/day}$  respectively. Figure 1.11 shows various

Ion-ion interaction



Ion-polar interaction



Ion-nonpolar interaction

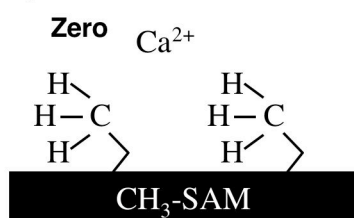


**Figure 1.11.** Various interaction modes between calcium and phosphate ions and surface functional groups as an initial step for hydroxyapatite formation. [3]

**Chapter 1**

interaction modes between calcium and phosphate ions and surface functional groups at an initial step for hydroxyapatite formation. The decrease in the growth rate could be attributed to the strength of interactions between calcium and phosphate ions and surface functional groups. Namely, negatively charged phosphate and carboxyl groups interact with  $Ca^{2+}$  ion electrostatically and then strongly induced hydroxyapatite formation. This finding indicated that hydroxyapatite formation was dominantly initiated via calcium ion-adsorption upon complexation with a negative surface-charged group.

On the basis of this report, amino acids contained in sericin and fibroin were classified into 5 groups, carboxyl, amide, hydroxyl, amino and hydrophobic containing groups, as given on Table 1.4. Sericin contains approximately 20 mol% of COOH group, whereas fibroin contains only 3 mol%. It should be noted that sericin contains approximately 44 mol% of OH group. However, the growth rate of hydroxyapatite on COOH containing surface were more than 10 times higher than that

**Table 1.4.** Classification of amino acids in sericin and fibroin based on the functional groups in side chain

<b>Rate of apatite formation</b>	<b>COOH &gt;&gt;</b>	<b>CONH<sub>2</sub> ≈</b>	<b>OH &gt;</b>	<b>NH<sub>2</sub> &gt;&gt;</b>	<b>Hydrophobic</b>
Amino acid	Glutamic acid Aspartic acid	Serine Threonine Tyrosine	Lysine Arginine Histidine	Glycine, Alanine Valine, Leucine Proline, Isoleucine Phenylalanine, Cystein, Methionine	
<b>Content / mol%</b>					
Sericin	19.64	43.62	7.41	23.35	
Fibroin	3.3	17.9	1.1	77.93	

on OH containing surface according to the report of Tanahashi *et al.*. Therefore, the contribution of the amino acids containing OH groups to induction of hydroxyapatite nucleation on sericin can be excluded. This indicated that carboxyl groups in aspartic acid and glutamic acid dominantly induced hydroxyapatite nucleation on sericin. This means that polypeptides rich in carboxyl groups may act as template substances to induce the deposition of hydroxyapatite crystals.

It is also noted that treatment with  $\text{CaCl}_2$  solutions at concentrations of 1 M or more is effective in increasing the rate of hydroxyapatite deposition on R-silk surface. Incorporation of a high concentration of  $\text{CaCl}_2$  with sericin on the R-silk surface may lead to acceleration in heterogeneous nucleation of hydroxyapatite by the release of  $\text{Ca}^{2+}$  ions from the fibers into the surrounding solution. The release of  $\text{Ca}^{2+}$  ions from the fiber increases the degree of supersaturation of the surrounding solution with respect to the hydroxyapatite. The increased degree of supersaturation supports a catalytic effect of the carboxyl groups for heterogeneous nucleation of the hydroxyapatite on sericin. Takadama *et al.* reported that silanol groups provide a nucleation site for hydroxyapatite formed from amorphous calcium silicate compounds comprising  $\equiv\text{SiOCa}^+$  and  $(\equiv\text{SiO})_2\text{Ca}$ , by incorporation of calcium ions before the hydroxyapatite deposition [24]. In the case of carboxyl groups, such complexes as  $-\text{COOCa}^+$  and  $(-\text{COO})_2\text{Ca}$  can be formed on the materials' surface, as shown in Figure 1.12. Prior treatment with an aqueous solution containing  $\text{Ca}^{2+}$  ions may increase the number of  $-\text{COOCa}^+$  and  $(-\text{COO})_2\text{Ca}$  complexes, even before immersion in 1.5SBF. This would make it easy for hydroxyapatite deposition to occur following immersion in biomimicking solutions such as 1.5SBF.

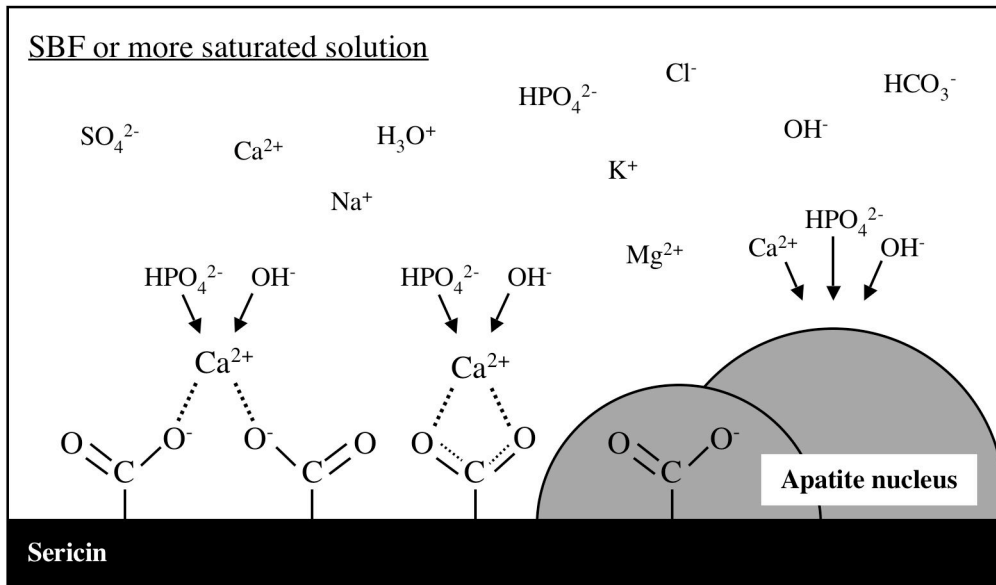


**Figure 1.12.** Mechanism of hydroxyapatite nucleation on sericin surface.

## 5. Conclusion

Sericin, a protein derived from silkworm, has the potential to induce hydroxyapatite deposition on its surface in biomimicking solutions such as 1.5SBF. The inducement of hydroxyapatite nucleation may be attributed to the existence of carboxyl groups on sericin. Hydroxyapatite formation on sericin can be accelerated by prior treatment with an aqueous solution containing calcium ions, such as a  $\text{CaCl}_2$  solution, having a concentration of 1 M or more. These findings support the proposition that novel organic–inorganic hybrids can be produced under biomimetic conditions utilizing a raw silk fiber rich in carboxyl groups as a substrate for the deposition of hydroxyapatite crystals.

## References

- [1] Abe Y, Kokubo T, Yamamuro T. Apatite coating on ceramics, metals and polymers utilizing a biological process. *J Mater Sci Mater Med* 1990;1:233-238.
- [2] Tanahashi M, Yao T, Kokubo T, Minoda M, Miyamoto T, Nakamura T, Yamamuro T. Apatite coating on organic polymers by a biomimetic process. *J Am Ceram Soc* 1994;77:2805-2808.
- [3] Tanahashi M, Matsuda T. Surface functional group dependence on apatite formation on self-assembled monolayers in a simulated body fluid. *J Biomed Mater Res* 1997;34:305-315.
- [4] Miyazaki T, Ohtsuki C, Akioka Y, Tanihara M, Nakao J, Sakaguchi Y, Konagaya S. Apatite deposition on polyamide film containing carboxyl group in a biomimetic solution. *J Mater Sci Mater Med* 2003;14:569-574.
- [5] Kawai T, Ohtsuki C, Kamitakahara M, Miyazaki T, Tanihara M, Sakaguchi Y, Konagaya S. Coating of an apatite layer on polyamide films containing sulfonic groups by a biomimetic process. *Biomaterials* 2004;25:4529-4534.
- [6] Furuzono T, Ishihara K, Nakabayashi N, Tamada Y. Chemical modification of silk fibroin with 2-methacryloxyethyl phosphorylcholine. II. Graft-polymerization onto fabric through 2-methacryloxyethyl isocyanate and interaction between fabric and platelets. *Biomaterials* 2000;21:327-333.
- [7] Furuzono T, Taguchi T, Kishida A, Akashi M, Tamada Y. Preparation and characterization of apatite deposited on silk fabric using an alternate soaking process. *J Biomed Mater Res* 2000;50:344-352.
- [8] Altman GH, Daiz F, Jakuba C, Calabro T, Horan RL, Chen J, Lu H,

- Richmond J, Kaplan DL. Silk-based biomaterials. *Biomaterials* 2003;24:401-416.
- [9] Furuzono T, Kishida A, Tanaka J. Nano-scaled hydroxyapatite/polymer composite I. Coating of sintered hydroxyapatite particles on poly( $\gamma$ -methacryloxypropyl trimethoxysilane)-grafted silk fibroin fibers through chemical bonding. *J Mater Sci Mater Med* 2004;15:19-23.
- [10] Furuzono T, Yasuda S, Kimura T, Kyotani S, Tanaka J, Kishida A. Nano-scaled hydroxyapatite/polymer composite IV. Fabrication and cell adhesion properties of a three-dimensional scaffold made of composite material with silk fibroin substrate to develop a percutaneous device. *J Artif Organs* 2004;7:137-144.
- [11] Tamada Y. Addition of new functions to silk proteins by chemical modification and their applications. *Bio Industry* 2004;21:54-60 [in Japanese].
- [12] Tsujimoto K, Takagi H, Takahashi M, Yamada H, Nakamori S. Cryoprotective effect of the serine-rich repetitive sequence in silk protein sericin. *J Biochem* 2001;129:979-986.
- [13] Zhang YQ. Applications of natural silk protein sericin in biomaterials. *Biotechnology Advances* 2002;20:91-100.
- [14] Terada S, Nishimura T, Sasaki M, Yamada H, Miki M. Sericin, a protein derived from silkworms, accelerates the proliferation of several mammalian cell lines including a hybridoma. *Cytotechnology* 2002;40:3-12.
- [15] Takahashi M, Tsujimoto K, Yamada H, Takagi H, Nakamori S. The silk protein, sericin protects against cell death caused by acute serum deprivation



- in insect cell culture. *Biotech Lett* 2003;25:1805-1809.
- [16] Tsujimoto K. Development of the functional fabric using the silk protein. *Bio Industry* 2004;21:46-53 [in Japanese].
- [17] Sasaki M, Kato Y, Yamada H, Terada S. Development of a novel serum-free freezing medium for mammalian cells using the silk protein sericin. *Biotechnol Appl Biochem* 2005;42:183-188.
- [18] Ohtsuki C, Kokubo T, Takatsuka K, Yamamuro T. Compositional dependence of bioactivity of glasses in the system CaO-SiO<sub>2</sub>-P<sub>2</sub>O<sub>5</sub>: Its *in vitro* evaluation. *J Ceram Soc Japan (Seramikkusu Ronbunshi)* 1991;99:1-6.
- [19] Ohtsuki C, Kushitani H, Kokubo T, Kotani S, Yamamuro T. Apatite formation on the surface of Ceravital-type glass-ceramic in the body. *J Biomed Mater Res* 1991;25:1363-1370.
- [20] Li P, Ohtsuki C, Kokubo T, Nakanishi K, Soga N, deGroot K. The role of hydrated silica, titania and alumina in inducing apatite on implants. *J Biomed Mater Res* 1994;28:7-15.
- [21] Kokubo T, Kim HM, Kawashita M, Takadama H, Miyazaki T, Uchida M, Nakamura T. Nucleation and growth of apatite on amorphous phases in simulated body fluid. *Glastech Ber Sci Technol* 2000;73C1:247-254.
- [22] Komatsu K. Chemical and structural characteristics of wild cocoon and silk. In: Hojo N, editor. *Structure of silk yarn, Part B: Chemical structure and processing of silk yarn*. Science Publishers, Inc: Enfield (NH); 2000. p 21-46.
- [23] Shimura K, Katagata Y. Chemical Structure of Silk Fibroin. In: Hojo N, editor. *Structure of silk yarn, Part B: Chemical structure and processing of silk yarn*. Science Publishers, Inc: Enfield (NH); 2000. p 3-20.

- [24] Takadama H, Kim HM, Kokubo T, Nakamura T. Mechanism of apatite formation induced by silanol groups: TEM observation. J Ceram Soc Japan 2000;108:118-121.

## **Chapter 2**

### **Formation of Hydroxyapatite on Silk Sericin in a Solution Mimicking Body Fluid: Structural Effect of Sericin**

#### **1. Introduction**

Bone and tooth are composites with a unique structure: nano-crystalline hydroxyapatite is packed and aligned cooperatively between organic matrices, such as collagen and some acidic proteins. This structure is constructed as a result of mineralization in a living body, a process known as biomineralization. During mineral formation, the organic matrix plays an important role, as it controls the location and organization of nucleation sites, and structure and orientation of hydroxyapatite [1]. It was proposed that noncollagenous proteins that bind to hydroxyapatite crystals in bone and tooth have precise calcium-binding sites dictated by the structure of the proteins such as  $\alpha$  helix and  $\beta$  sheet [2,3]. These phenomena provide us with a hypothesis: an arrangement of functional groups that induce heterogeneous nucleation of hydroxyapatite must be important for effective nucleation of hydroxyapatite, as well as an existence of the functional groups.

A biomimetic process utilizing a simulated body fluid (SBF) or more

saturated solutions such as 1.5SBF, that has 1.5 times ion concentrations of SBF, has focused attention on coating of hydroxyapatite onto organic polymers [4,5]. To achieve a coating of hydroxyapatite, the existence of specific functional groups that induce heterogeneous nucleation of hydroxyapatite, such as silanol, carboxyl, and phosphate groups, on organic polymer surfaces is required [6-8]. However, the arrangement of functional groups on organic polymer surfaces has not been well considered.

This study focused on examining the structural effect of silk sericin on hydroxyapatite formation in 1.5SBF. In Chapter 1, it was shown that sericin had an ability to induce hydroxyapatite nucleation effectively in 1.5SBF. Sericin may be a suitable organic polymer to study structural effect on hydroxyapatite deposition because its molecular weight and secondary structure can be easily changed [9-12]. In this Chapter, sericin films with different structures were prepared, and their ability to form hydroxyapatite in 1.5SBF was examined.

## **2. Experimental procedure**

### **2.1. Preparation of sericin**

Four types of sericin solutions were prepared under different conditions. Preparation conditions and abbreviated name of sericins were summarized in Table 2.1. The solutions were prepared by the degummed raw silk fiber of *Bombyx mori* in ultra-pure water without any agents such as sodium carbonate to avoid contaminations. The degumming process was performed using an autoclave (SV-302 II, Advantec Toyo, Ltd., Japan) at either 105 or 120°C for 1 hour. Some of the samples were stored at 4°C for 2 weeks.

**Table 2.1.** Preparation conditions for sericin solutions

<b>Notations</b>	<b>Extraction</b>	<b>Storage</b>
105-0d	105°C, 1 hour	0 day
120-0d	120°C, 1 hour	0 day
105-2w	105°C, 1 hour	2 weeks
120-2w	120°C, 1 hour	2 weeks

## **2.2. Characterization of samples**

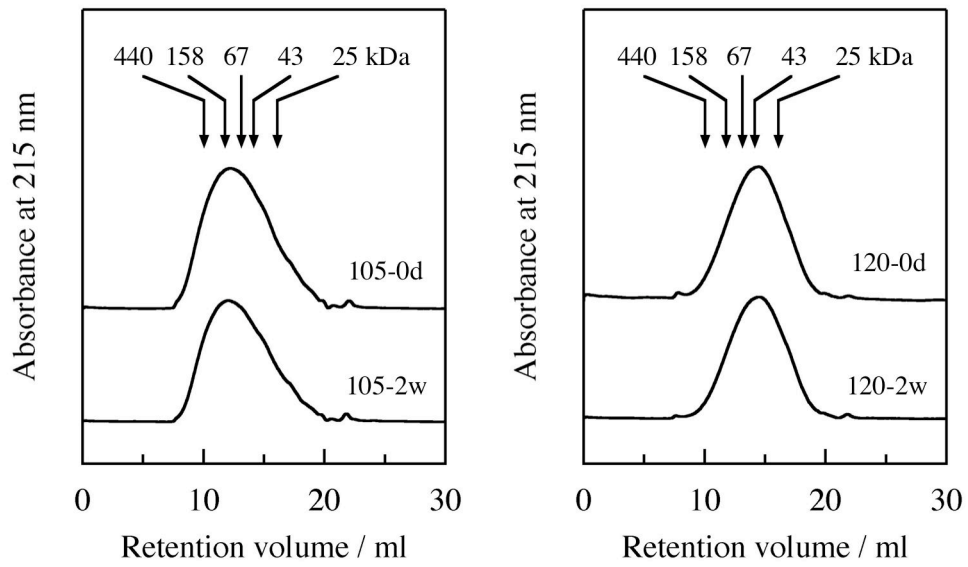
Molecular weights of the sericins were determined using gel permeation chromatography (GPC) employing an ÄKTA purifier system (Amersham Biosciences Corp., NJ, USA), using the following experimental parameters: column = Superdex 200 HR 10/30, elution buffer = 10 mM phosphate buffer containing 150 mM NaCl (PBS, pH = 7.4), flow rate = 0.5 mL/min, and detection wavelength = 215 nm. The peak molecular weight was calculated from a standard curve obtained using an Amersham Biosciences gel filtration calibration kit. The concentration of sericin in the extracted solution was determined using a bicinchoninic acid (BCA) protein assay kit (Pierce, Rockford, IL, USA). The solution was diluted with ultra-pure water to a concentration of approximately 0.3 mg/mL. Then, 0.3 mg/mL of the sericin solution was analysed using circular dichroism (CD) spectroscopy (J-820, JASCO, Japan). The sericin films were fabricated onto a polyethylene film by drying solutions containing 6 mg/mL of sericin. The sericin layer on the polyethylene film was analyzed using Fourier transform infrared (FT-IR) spectroscopy (Spectrum One, Perkin Elmer Ltd., UK).

### 2.3. Soaking in 1.5SBF

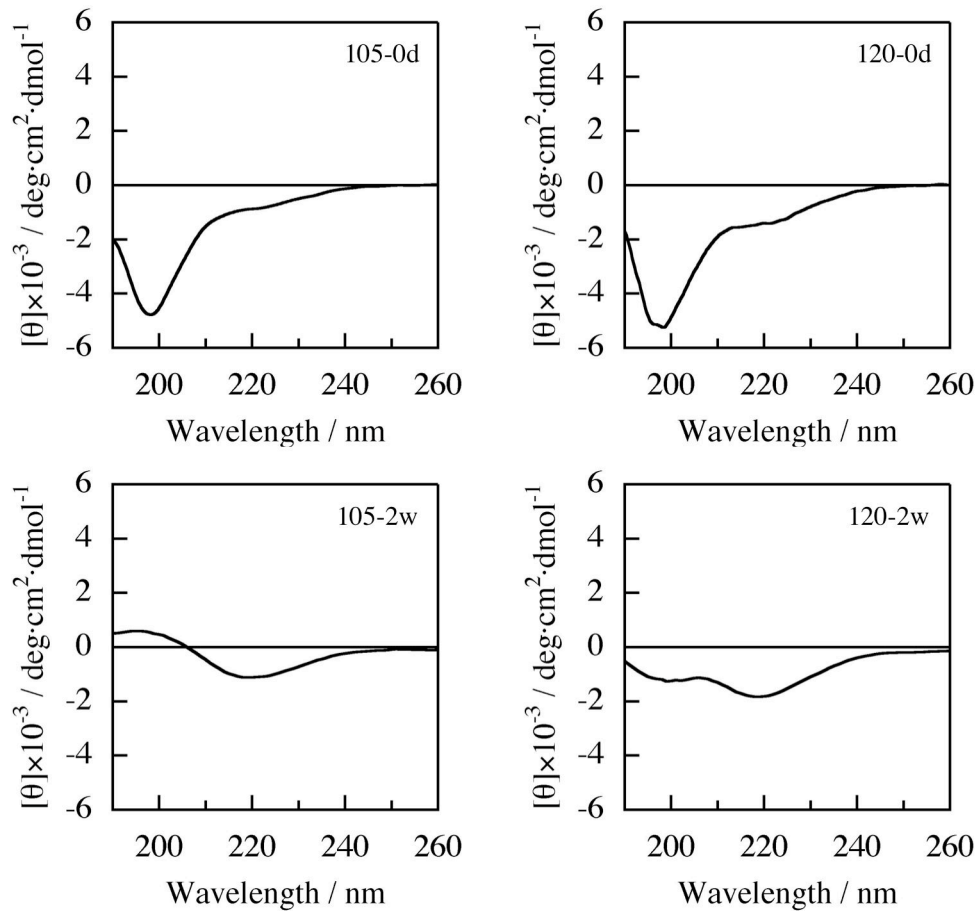
Films were prepared by casting the solution in a Petri dish (diameter = 60 mm, height = 15 mm) to form a thin sericin film on the bottom of the dish. The cast films were exposed to 1.5SBF. The solution was buffered at pH = 7.25 using 75 mol·m<sup>-3</sup> of tris(hydroxymethyl) aminomethane, along with an appropriate volume of hydrochloric acid, following the method reported by Kokubo *et al.* [2]. The temperature of the solution was maintained at 36.5°C. A volume of 15 mL of 1.5SBF was poured into a Petri dish coated with a sericin film, and kept for 7 days at 36.5°C. The films were observed both before and after soaking in 1.5SBF using a scanning electron microscope (SEM, S-3500N, Hitachi Ltd., Japan). In the SEM observations, the surfaces of some of the samples were coated with a sputtered gold film. The surfaces of the films were characterized using thin-film X-ray diffraction (TF-XRD, MXP3V, MAC Science Ltd., Japan). In the TF-XRD apparatus, the incident beam was set at an incident angle of 1° against the sample surface.

### 3. Results

Figure 2.1 shows the GPC profiles of sericins extracted under various conditions. The most frequent distribution in the molecular weight appeared at approximately 159 kDa and 43 kDa for Samples 105-0d and 120-0d, respectively. The sericin samples stored at 4°C for 2 weeks showed molecular weights, 141 and 37 kDa respectively, and they were almost equal to those of the as-prepared sericins. Figure 2.2 shows the CD spectra of these sericin samples. The CD spectrum of 105-0d was assigned as a random coil structure from a negative cotton band occurring near to 198 nm [13-16]. After storage for two weeks storage at 4°C, the intensity of the band at 198 nm decreased and a positive cotton band were detected.



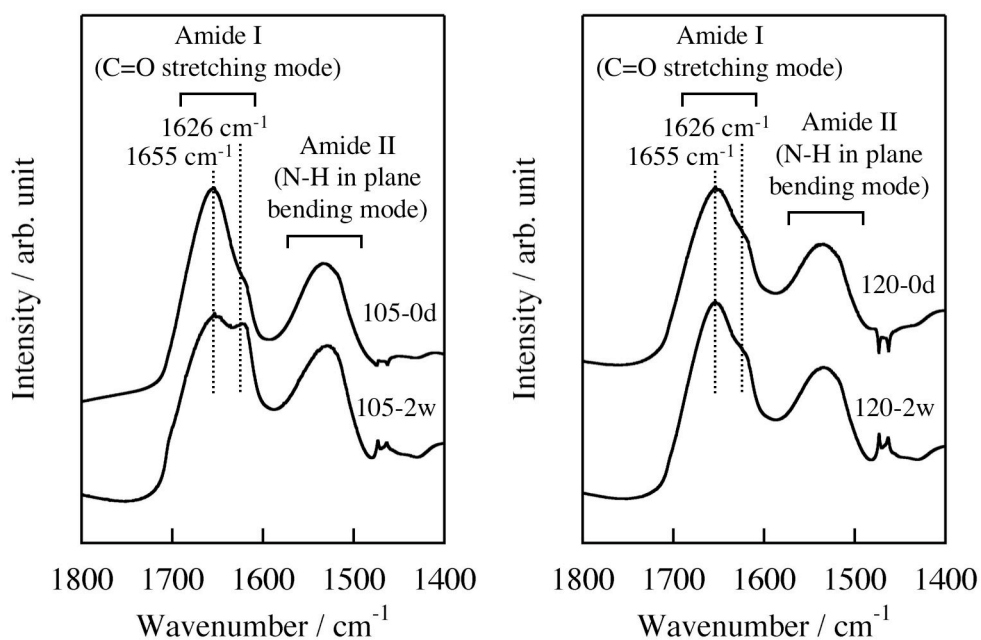
**Figure 2.1.** GPC profiles of sericins extracted under various conditions.



**Figure 2.2.** CD spectra of sericin solutions extracted under various conditions.

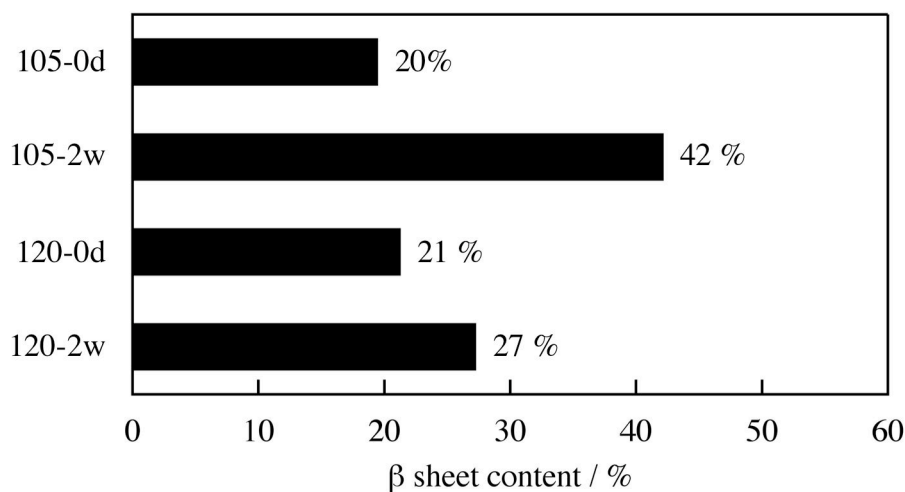
This shows that the content of  $\beta$  sheet structure of sericin increased during storage of the solution. The behavior of the sericin extracted at  $120^{\circ}\text{C}$  was similar to that of the sericin extracted at  $105^{\circ}\text{C}$ . However, the content of  $\beta$  sheet structure in 105-2w was higher than that in 120-2w.

Figure 2.3 shows the FT-IR spectra of the sericin films. The two absorption bands located at  $1655$  and  $1550\text{ cm}^{-1}$  were assigned to the amide I ( $\nu\text{C}=\text{O}$ ) and amide II ( $\delta\text{N}-\text{H}$ ) stretches, respectively. The absorption peak located at  $1655\text{ cm}^{-1}$  was attributed to a random coil structure [17]. A shoulder peak located at  $1626\text{ cm}^{-1}$  was attributed to a  $\beta$  sheet structure. The intensity of the latter peak was significantly higher for the film prepared using 105-2w than for the film prepared using 105-0d. This tendency was also observed for films prepared from sericin extracted at  $120^{\circ}\text{C}$ . However, the increase in intensity was less than that detected in



**Figure 2.3.** FT-IR spectra of sericin films prepared from sericin solutions extracted under various conditions.





**Figure 2.4.** β sheet contents in sericin films .

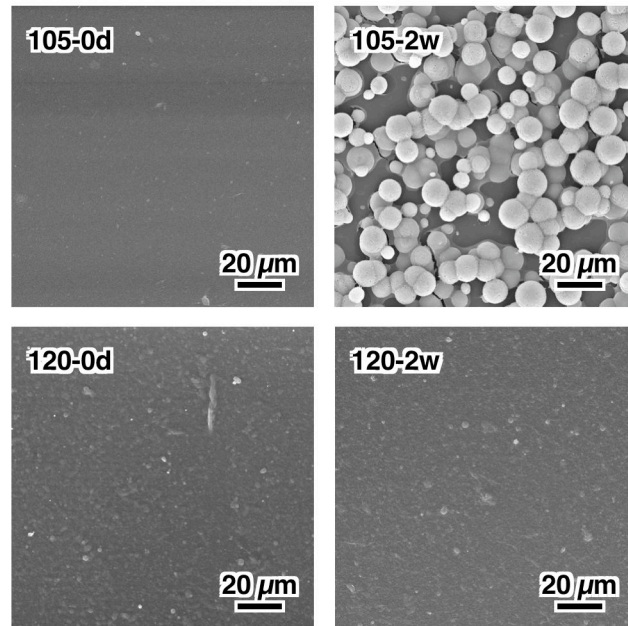
the spectra of films prepared from sericin extracted at 105°C. These results indicate that a random coil structure is dominant in sericin films prepared immediately after extraction. The proportion of β sheet structure increased during ageing at 4°C, and the proportion of the β sheet structure in sericin extracted at 105°C was higher than that in sericin extracted at 120°C. Figure 2.4 shows β sheet contents in sericin films calculated from the ratio of assigned peak area in amide I region. The peak assignment was done via Gaussian curve-fitting using Igor Pro (Wave Metrics, Inc.). The content of β sheet in the film of 105-2w was approximately 42 % and it was the highest than the other films.

Figure 2.5 shows SEM images of the surfaces of sericin films soaked in 1.5SBF for 7 days. Among the films prepared from the extracted sericin, only the film prepared from 105-2w had particles deposited on its surface. On the surfaces of the films prepared from the other sericins, any changes in their morphology were not observed. The FT-XRD patterns of the sericin films soaked in 1.5SBF for 7 days are shown in Figure 2.6. A broad peak assigned to hydroxyapatite was detected only in the film prepared from 105-2w after soaking in 1.5SBF. These results confirm that the particles formed on the film after soaking in 1.5SBF were hydroxyapatite.

#### 4. Discussion

From the results described above, hydroxyapatite deposition was not observed in all the sericin films, but was observed only for a certain type of sericin film. Deposition of hydroxyapatite on a substrate in 1.5SBF is initiated by the existence of a substance that can induce heterogeneous nucleation of hydroxyapatite. Therefore, only the sericin film prepared from 105-2w had the potential to induce heterogeneous nucleation of hydroxyapatite. The CD and FT-IR spectra data showed that the film made from 105-2w had the highest content of  $\beta$  sheet structure among the prepared sericin films. The higher molecular weight of 105-2w than 120-2w may enable the sericin to form higher content of  $\beta$  sheet. These results indicate that sericin film with high content of  $\beta$  sheet structure produce an effective surface for hydroxyapatite formation.

Previous studies have reported that hydroxyapatite deposition can be initiated by functional groups existing on the surface of a material [6-8]. Carboxyl groups are effective for nucleation of hydroxyapatite in solutions that mimic body fluid [8]. Nucleation of hydroxyapatite on sericin film surface must be induced by



**Figure 2.5.** SEM images of the surfaces of sericin films after soaking in 1.5SBF for 7 days.

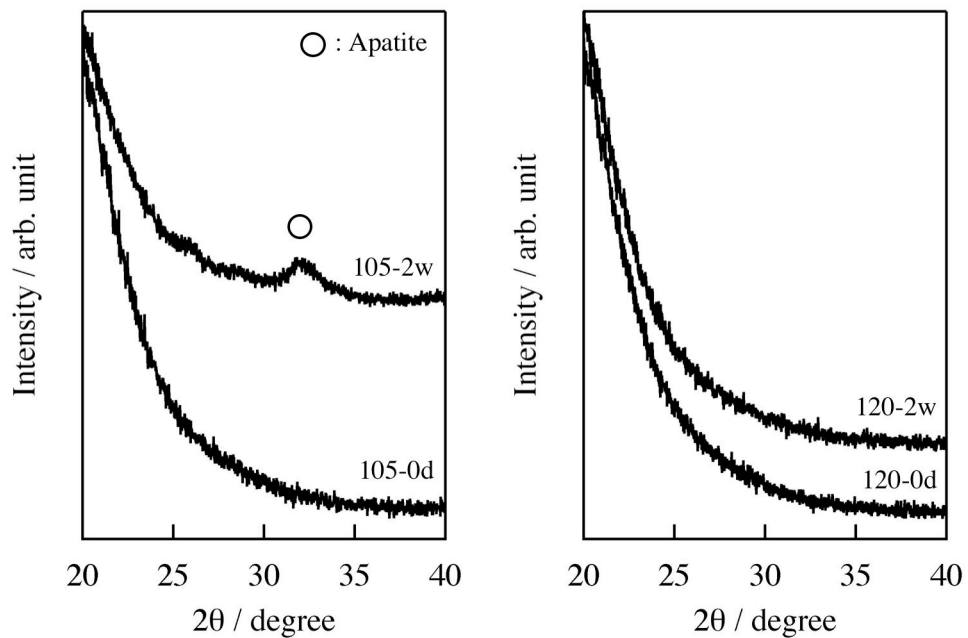


**Figure 2.6.** TF-XRD patterns of the surfaces of sericin films after soaking in 1.5SBF for 7 days.

carboxyl groups contained in acidic amino acids in sericin [18], as shown in Chapter 1. Interestingly, the results of this study indicated that heterogeneous nucleation of hydroxyapatite on sericin is governed by its secondary structure as well as the existence of carboxyl groups. When a protein has a  $\beta$  sheet structure, functional groups of side chains in amino acids generally point above and below the  $\beta$  sheet alternately [19]. The  $\beta$  sheet structure in sericin molecules allows an orientation of carboxyl groups, whereas the random coil does not. Namely, about half amount of the carboxyl groups in sericin can be arranged perpendicular to the sheet when the sericin has an ideal  $\beta$  sheet structure, as shown in Figure 2.7. Such a specific arrangement of the functional groups would provide the sites that are suitable for hydroxyapatite nucleation. Consequently, hydroxyapatite nucleation on a substrate in a solution mimicking body fluid is very sensitive to such structural arrangements of functional groups. This finding is useful for the design of organic polymers that

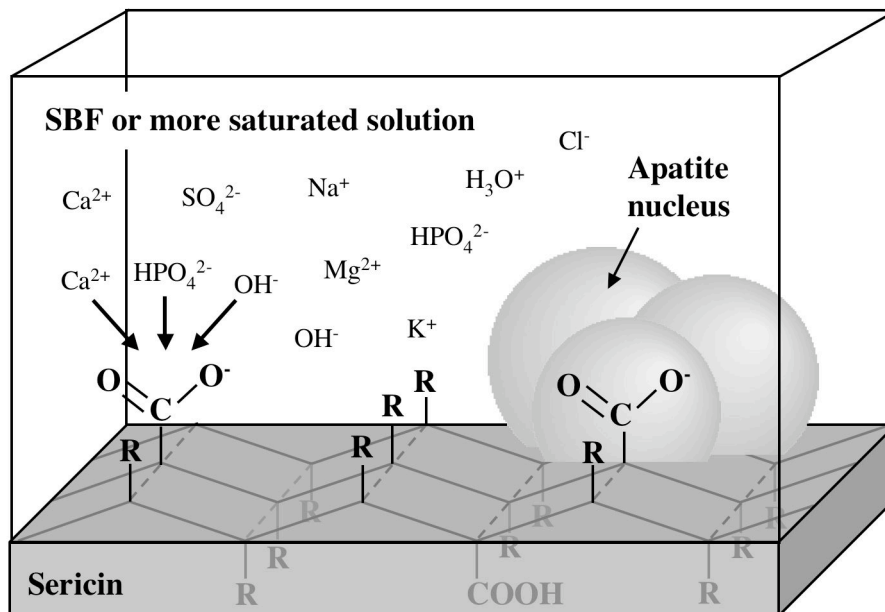


**Figure 2.7.** Mechanism of hydroxyapatite nucleation on sericin substrate with  $\beta$  sheet structure in SBF or more saturated solutions.

can effectively induce hydroxyapatite nucleation.

## **5. Conclusion**

Sericin, a protein derived from silkworm, can induce hydroxyapatite deposition on its surface in a solution mimicking body fluid, when it has a high content of  $\beta$  sheet structure. This indicates that the induction of hydroxyapatite nucleation is governed by the arrangement of carboxyl groups on the protein. This finding is valuable to design novel organic polymers for preparing hybrid materials.

## **References**

- [1] Mann S. In: Compton RG, Davies SG, Evans J, editors. *Biom mineralization*. New York: Oxford University Press, Inc.; 2001. p. 89-124.
- [2] Hoang QQ, Sicheri F, Howard AJ, Yang DSC. Bone recognition mechanism of porcine osteocalcin from crystal structure. *Nature* 2003;425:977-980.
- [3] He G, Dahl T, Veis A, George A. Nucleation of apatite crystals in vitro by self-assembled dentin matrix protein 1. *Nature materials* 2003;2:552-559.
- [4] Abe Y, Kokubo T, Yamamuro T. Apatite coating on ceramics, metals and polymers utilizing a biological process. *J Mater Sci Mater Med* 1990;1:233-238.
- [5] Tanahashi M, Yao T, Kokubo T, Minoda M, Miyamoto T, Nakamura T, Yamamuro T. Apatite coating on organic polymers by a biomimetic process. *J Am Ceram Soc* 1994;77:2805-2808.

- [6] Li P, Ohtsuki C, Kokubo T, Nakanishi K, Soga N, Nakamura T, Yamamuro T. Apatite formation induced by silica gel in a simulated body fluid. *J Am Ceram Soc* 1992;75:2094-2097.
- [7] Li P, Ohtsuki C, Kokubo T, Nakanishi K, Soga N, de Groot K. The role of hydrated silica, titania and alumina in inducing apatite on implants. *J Biomed Mater Res* 1994;28:7-15.
- [8] Tanahashi M, Matsuda T. Surface functional group dependence on apatite formation on self-assembled monolayers in a simulated body fluid. *J Biomed Mater Res* 1997;34:305-315.
- [9] Komatsu K. Chemical and structural characteristics of silk sericin. In: Hojo N, editor. *Structure of silk yarn, Part B: Chemical structure and processing of silk yarn*. Science Publishers, Inc: Enfield (NH); 2000. p. 47-85.
- [10] Takasu Y, Yamada H, Tsubouchi K. Isolation of three main sericin components from the cocoon of the silkworm, *Bombyx mori*. *Biosci Biotechnol Biochem* 2002;66:2715-2718.
- [11] Lee KG, Kweon HY, Yeo JH, Woo SO, Lee YW, Cho CS, Kim KH, Park YH. Effect of methyl alcohol on the morphology and conformational characteristics of silk sericin. *Int J Biol Macromol* 2003;33:75-80.
- [12] Tsujimoto K. Development of the functional fabric using the silk protein. *Bio Industry* 2004;21:46-53 [in Japanese].
- [13] Brahms S, Brahms J. Determination of protein secondary structure in solution by vacuum ultraviolet circular dichroism. *J Mol Biol* 1980;138:148-178.
- [14] Madson V, Schellman J. Optical activity of polypeptides and proteins.

- Biopolymers 1972;11:1041-1076.
- [15] Greenfield N, Fasman GD. Computed circular dichroism spectra for the evaluation of protein conformation. *Biochemistry* 1969;8:4108-4116.
- [16] Townend R, Kumosinski TF, Timasheff SN, Fasman GD, Davidson B. The circular dichroism of the  $\beta$ -structure of poly-L-lysine. *Biochem Biophys Res Comm* 1966;23:163-169.
- [17] Miyazawa T, Blout ER. The infrared spectra of polypeptides in various conformations: amide I and II bands. *J Am Chem Soc* 1961;83:712-719.
- [18] Komatsu K. Chemical and structural characteristics of wild cocoon and silk. In: Hojo N, editor. *Structure of silk yarn, Part B: Chemical structure and processing of silk yarn*. Science Publishers, Inc: Enfield (NH); 2000. p 21-46.
- [19] Branden C, Tooze J. In: *Introduction to protein structure*. New York: Garland Publishing, Inc.; 1999. p 13-34.

## **Chapter 3**

### **Formation of Hydroxyapatite on Synthetic Polypeptide in a Solution Mimicking Body Fluid**

#### **1. Introduction**

Hydroxyapatite coating on organic polymers is an appealing way to develop hybrid materials for medical applications. The biomimetic process has been focused attention on fabricating such hybrids where a hydroxyapatite layer can be coated onto organic substrates, either by using a simulated body fluid (SBF) with ion concentrations nearly equal to those of human blood plasma or more concentrated solutions such as 1.5SBF, that has 1.5 times the ion concentrations of SBF [1,2]. In order to achieve a successful coating of hydroxyapatite utilizing these solutions, it is necessary to find organic polymers that effectively induce hydroxyapatite nucleation. In Chapters 1, it was shown that sericin, a kind of silk protein, had an ability to effectively induce hydroxyapatite nucleation. It was shown in Chapter 2 that the ability of sericin containing a  $\beta$  sheet structure to induce hydroxyapatite nucleation was higher than that of sericin with a random coil structure. Specifically, sericin may provide an effective surface for hydroxyapatite nucleation due to the existence



of carboxyl groups and the formation of the  $\beta$  sheet structure. However, it is difficult to investigate these effects on hydroxyapatite nucleation in detail because sericin consists of many kinds of amino acids, such as serine. In this Chapter, therefore, synthesis of polypeptide containing carboxyl groups and  $\beta$  sheet structure was attempted. Hydroxyapatite formation on its surface was examined in order to confirm the effect of carboxyl groups and  $\beta$  sheet structure on the induction of heterogeneous nucleation of hydroxyapatite.

Xiong *et al.* [3] reported that peptides with alternating nonpolar and polar amino acid residues have a tendency to form a  $\beta$  sheet structure. According to this report, peptides consisting of 8 amino acid residues alternating polar/nonpolar amino acids were designed. As nonpolar amino acids, alanine (A), valine (V), leucine (L) and phenylalanine (F) were selected. Levitt [4] reported that these amino acids have different preferences for  $\alpha$  helix and  $\beta$  sheet, as shown on Table 3.1. In particular, valine and phenylalanine favor  $\beta$  sheet formation because of the bulky side chains,  $\beta$  branched alkyl group and phenyl group (Figure 3.1). Therefore, the peptides containing valine and phenylalanine are expected to form a  $\beta$  sheet structure. On the other hand, alanine and leucine favor  $\alpha$  helix. The peptides containing alanine and leucine are, therefore, expected to have less content of  $\beta$  sheet than the peptides containing valine and phenylalanine. As a polar amino acid, glutamic acid (E) was selected. Glutamic acid contains a carboxyl group in the side chain and it is expected to induce hydroxyapatite nucleation in a solution mimicking body fluid. As a control, a peptide that does not contain carboxyl groups in the side chain, the peptide containing glutamine (Q), instead of glutamic acid, was also synthesized. The amino acid sequences of peptides synthesized in this Chapter are summarized in Table 3.2. As a residue at C-terminal of peptides, glycine, which is

indifferent to racemization occurring during peptide synthesis, was selected. In this Chapter, these peptides were prepared. Their hydroxyapatite-forming ability in 1.5SBF was investigated.

**Table 3.1.** Conformational preferences of amino acids for  $\alpha$  helix and  $\beta$  sheet

<b>Amino acid</b>	<b><math>\alpha</math> helix</b>	<b><math>\beta</math> sheet</b>
Alanine, A	favoring	indifferent
Valine, V	indifferent	favoring
Leucine, L	favoring	indifferent
Phenylalanine, F	indifferent	favoring

**Table 3.2.** Peptides synthesized in this study

<b>Peptide</b>	<b>Amino acid sequence</b>
(AE) <sub>3</sub> AG	AEAEAEAG
(VE) <sub>3</sub> VG	VEVEVEVG
(LE) <sub>3</sub> LG	LELELELG
(LQ) <sub>3</sub> LG	LQLQLQLG
(FE) <sub>3</sub> FG	FEFEFEFG
(FQ) <sub>3</sub> FG	FQFQFQFG

A: Alanine, V: Valine, L: Leucine, F: Phenylalanine  
E: Glutamic acid, Q: Glutamine

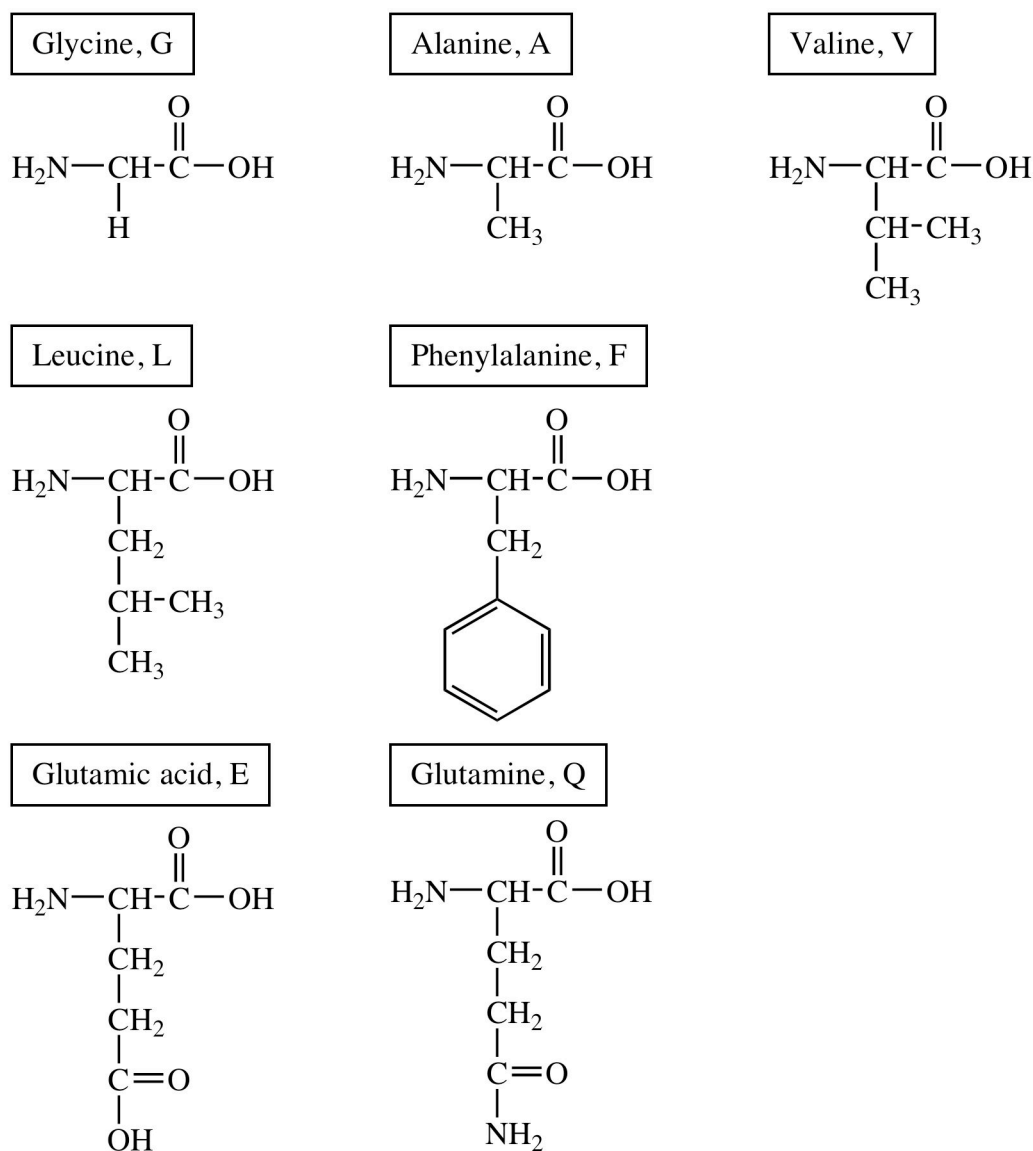


**Figure 3.1.** Structural formulae of amino acids.

## 2. Experimental procedure

### 2.1. Preparation of peptides

The peptides were prepared using an ABI-433A Peptide Synthesizer (Applied Biosystems, CA, USA) using solid-phase Fmoc chemistry. They were cleaved from the resin with either trifluoroacetic acid (TFA, Peptide Institute, Inc.,

Osaka, Japan) containing 5% water or TFA containing 2.5% ethanedithiol and 2.5% water. The obtained peptides were used without purification because the peptides, except for (AE)<sub>3</sub>AG, were poorly soluble in water. The secondary structures of the peptides were determined by circular dichroism (CD) spectroscopy using a J-820 spectrometer (JASCO, Japan). The peptide of (AE)<sub>3</sub>AG was dissolved to the concentration of 0.3 mg/mL in ultra-pure water. The other peptides were dissolved to the concentration of 0.6 mg/mL in 1,1,1,3,3,3-hexafluoro-2-propanol (HFIP, Wako Pure Chemicals, Osaka, Japan) and an equal volume of either ultra-pure water or HFIP was then added to obtain 0.3 mg/mL of peptide solutions in either HFIP/H<sub>2</sub>O= 1/1 or HFIP. Spectra were acquired at 25°C in a 1 mm cuvette.

## **2.2. Polymerization of peptides**

The peptides were polymerized in dimethyl sulfoxide (DMSO, MERCK, Tokyo, Japan) using diisopropylethylamine (DIPEA, Peptide Institute, Inc., Osaka, Japan), 1-hydroxybenzotriazol (HOBt, Peptide Institute, Inc., Osaka, Japan) and 1-ethyl 3-(3-dimethyl-aminopropyl) -carbodiimide (EDC·HCl, Peptide Institute, Inc., Osaka, Japan). The peptides were dissolved at the concentration of 10 mM in DMSO, to which was added an equivalent molar of DIPEA, HOBt, and 3 equivalent molars of EDC·HCl. The mixtures were kept at 20°C and stirred. After 48 hours, they were dialyzed in ultra-pure water to obtain aqueous solutions of polypeptides.

## **2.3. Characterization of polypeptides**

Molecular weights of the polypeptides were determined using gel permeation chromatography (GPC). The GPC analysis was carried out on an ÄKTA purifier system (Amersham Bioscience Corp., NJ, USA) using the following

experimental parameters: column = Superdex 200 HR 10/30, elution buffer = 10 mM phosphate buffer containing 15 mM NaCl (PBS, pH = 7.4), flow rate = 0.5 mL/min, and detection wavelength = 215 nm. The peak molecular weight was calculated from a globular protein standard curve obtained using an Amersham Biosciences gel filtration calibration kit. Since the polypeptides containing valine, leucine, phenylalanine were poorly soluble in the elution buffer, measurements of GPC in HFIP were also performed. The measurements were performed at Tosoh Analysis and Research Center (Japan) and the molecular weights were calculated from a standard curve obtained using polymethylmethacrylate (PMMA).

Secondary structures of polypeptides were determined using CD spectroscopy. The aqueous solutions containing the polypeptides were frozen at  $-30^{\circ}\text{C}$  and freeze-dried using a freeze dryer (FRD-82M, IWAKI (ASAHI Techno Glass), Tokyo, Japan). The resultant powders of polypeptides were dissolved at the concentration of 0.6 mg/mL in HFIP, and an equal volume of ultra-pure water or HFIP was added to obtain 0.3 mg/mL of polypeptide solutions in  $\text{H}_2\text{O}/\text{HFIP} = 1/1$  or in HFIP. For poly(AE)<sub>3</sub>AG, 5 mg/mL of solution in HFIP was also prepared and kept for 1 hour under ambient condition. The solution was diluted with HFIP to obtain 0.3 mg/mL of poly(AE)<sub>3</sub>AG solution in HFIP. Spectra were acquired at  $25^{\circ}\text{C}$  in a 1 mm cuvette. Secondary structures of polypeptides in forms of films were determined using CD and Fourier transform infrared (FT-IR) spectroscopy. For CD measurements, the solutions of polypeptides in  $\text{HFIP}/\text{H}_2\text{O} = 1/1$  or in HFIP were cast onto silica glass plates and dried under ambient conditions at  $40^{\circ}\text{C}$ . Spectra were acquired at  $25^{\circ}\text{C}$ . For FT-IR measurements, the polypeptide solutions obtained by dialysis after polymerization were cast onto a polyethylene film and then dried under ambient conditions at  $40^{\circ}\text{C}$ . Spectra were acquired using an FT-IR

spectrometer (Spectrum one, Elmer Ltd., UK).

Contact angle measurements were performed for polypeptide films formed on a polystyrene Petri dish. The contact angles were obtained by water droplets under ambient conditions using a standard contact angle apparatus (G-1 Contact Anglemeter, ERMA Inc., Japan).

#### **2.4. Soaking in 1.5SBF**

Polypeptide films were prepared by casting the solution on a Petri dish to form a polypeptide film on the bottom of the dish. The cast films were exposed to 15 mL of 1.5SBF ( $\text{Na}^+$  213.0,  $\text{K}^+$  7.5,  $\text{Mg}^{2+}$  2.3,  $\text{Ca}^{2+}$  3.8,  $\text{Cl}^-$  221.7,  $\text{HCO}_3^-$  6.3,  $\text{HPO}_4^{2-}$  1.5 and  $\text{SO}_4^{2-}$  0.8 mM). The solution was buffered at  $\text{pH} = 7.25$  using 75 mol/m<sup>3</sup> of tris-hydroxymethyl-aminomethane and appropriate amounts of hydrochloric acid, according to the method reported by Kokubo *et al.* [2]. After keeping at 36.5°C for various periods, the surface of the film was characterized using an electron scanning microscope (FE-SEM: S-4800 Hitachi Ltd., Japan) and a thin-film X-ray diffractometer (TF-XRD; RINT2200V/PC-LR, Rigaku Co., Japan).

### **3. Results**

Figure 3.2 shows the CD spectra of the peptides. The spectrum of (AE)<sub>3</sub>AG in H<sub>2</sub>O, showed a negative cotton band at 198 nm assigned to a random coil structure [5-8]. The spectra of the peptides other than (AE)<sub>3</sub>AG were measured in H<sub>2</sub>O containing HFIP because the peptides other than (AE)<sub>3</sub>AG were not soluble in H<sub>2</sub>O. For (VE)<sub>3</sub>VG and (FE)<sub>3</sub>FG, a positive cotton band at 197 nm and a negative cotton band at 217 nm assigned to a  $\beta$  sheet were detected. The peptides containing leucine residues, (LE)<sub>3</sub>LG and (LQ)<sub>3</sub>LG, showed a negative cotton band at 200 nm

and a negative shoulder at 220 nm were detected. These spectra indicate that peptides containing leucine residues form  $\alpha$  helix containing some amount of random coil structure. For (FQ)<sub>3</sub>FG, the spectrum could not be measured even in H<sub>2</sub>O containing HFIP. The CD spectra of the peptides other than (AE)<sub>3</sub>AG were also measured in HFIP. For all the peptides other than (AE)<sub>3</sub>AG, a negative cotton band at 198 nm assigned to random coil structure was detected. It was obvious that HFIP had prevented these peptides from forming specific secondary structures such as  $\alpha$  helix and  $\beta$  sheet. The dominant secondary structures of peptides estimated from the results of CD measurement are summarized in Table 3.3.

**Table 3.3.** Dominant structures of peptides in various solvent determined using CD spectroscopy

Peptide	In H <sub>2</sub> O	In HFIP/H <sub>2</sub> O=1/1	In HFIP
(AE) <sub>3</sub> AG	Random coil	-	-
(VE) <sub>3</sub> VG	NM	$\beta$ sheet	Random coil
(LE) <sub>3</sub> LG	NM	$\alpha$ helix / random coil	Random coil
(LQ) <sub>3</sub> LG	NM	$\alpha$ helix / random coil	Random coil
(FE) <sub>3</sub> FG	NM	$\beta$ sheet	Random coil
(FQ) <sub>3</sub> FG	NM	NM	Random coil

NM: Not measurable, -: Not measured  
A: Alanine, V: Valine, L: Leucine, F: Phenylalanine  
E: Glutamic acid, Q: Glutamine

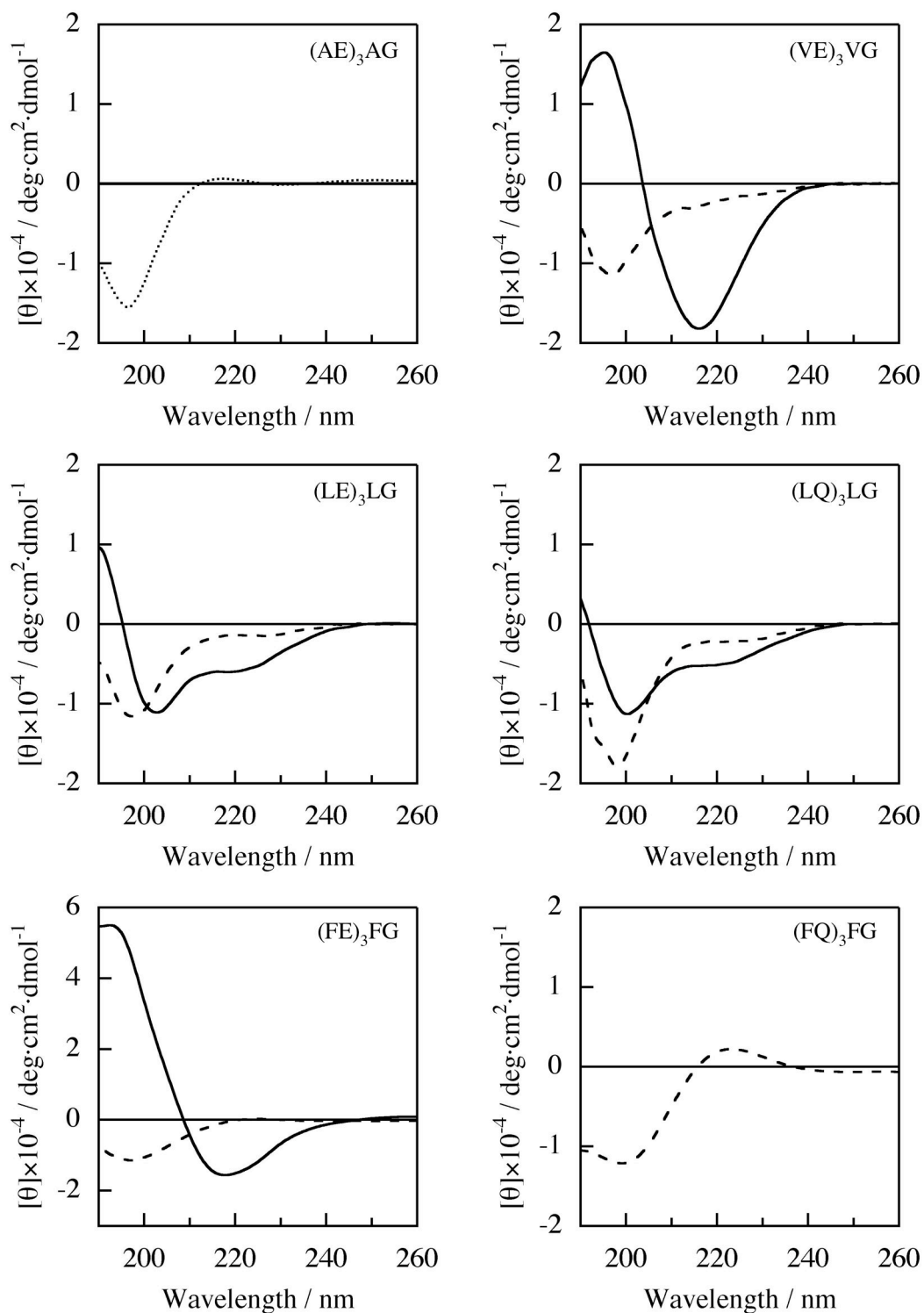


**Figure 3.2.** CD spectra of peptides.

.....: in H<sub>2</sub>O, —: in H<sub>2</sub>O/HFIP, - - - -: in HFIP,  
 HFIP: 1,1,1,3,3,3-hexafluoro-2-propanol, A: Alanine, V: Valine, L: Leucine,  
 F: Phenylalanine, E: Glutamic acid, Q: Glutamine



Table 3.4 shows the molecular weights of polypeptides. Poly(AE)<sub>3</sub>AG and poly(FE)<sub>3</sub>FG showed the highest frequency in the molecular weights of polypeptides appeared at approximately 25 kDa and 190 kDa, respectively, and poly(VE)<sub>3</sub>VG contained more than 669 kDa of polypeptide in PBS. These results were, however, detected some of polypeptides that can be dissolved in PBS. In the measurement for poly(LE)<sub>3</sub>LG, poly(LQ)<sub>3</sub>LG and poly(FQ)<sub>3</sub>FG, no peak assigned to polypeptides was detected. In HFIP, poly(VE)<sub>3</sub>VG showed 18000 of the molecular weight and poly(LE)<sub>3</sub>LG, poly(LQ)<sub>3</sub>LG, poly(FE)<sub>3</sub>FG and poly(FQ)<sub>3</sub>FG showed the molecular weights in the range of 6000 to 12000. Since the molecular weights in PBS were calculated from a standard curve obtained using globular proteins, they were higher than the values in HFIP that were calculated using PMMA. The higher molecular

**Table 3.4.** Molecular weights of polypeptides

Polypeptide	Molecular weight	
	In PBS	In HFIP
poly(AE) <sub>3</sub> AG	25 kDa	Not measured
poly(VE) <sub>3</sub> VG	> 669 kDa	18000
poly(LE) <sub>3</sub> LG	Not determined	6000
poly(LQ) <sub>3</sub> LG	Not determined	8600
poly(FE) <sub>3</sub> FG	190 kDa	7500
poly(FQ) <sub>3</sub> FG	Not determined	12000

A: Alanine, V: Valine, L: Leucine, F: Phenylalanine  
E: Glutamic acid, Q: Glutamine

weights in PBS must be also caused by the aggregation of polypeptide in PBS.

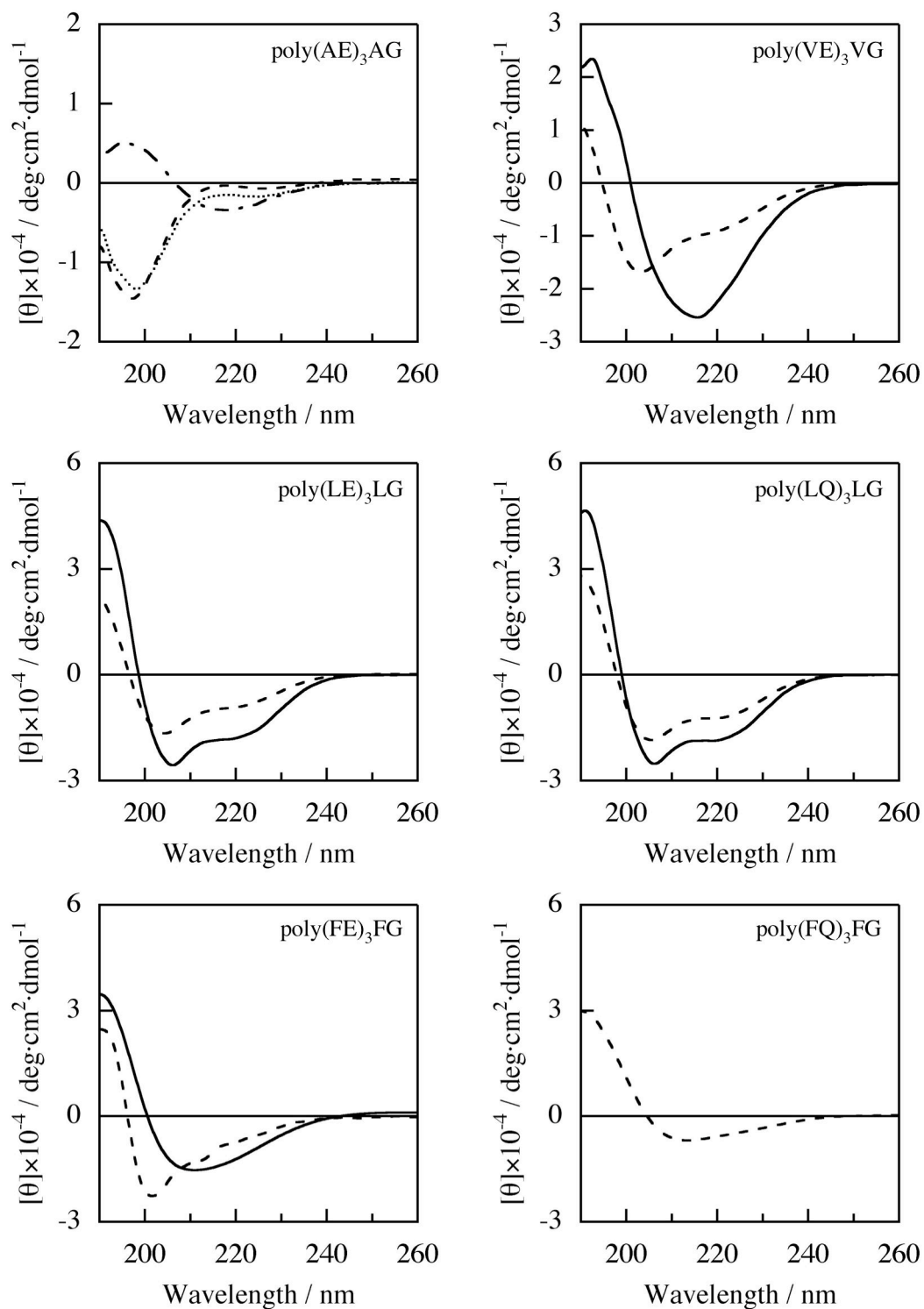
Figure 3.3 shows the CD spectra of polypeptides. The structures of polypeptides determined from these spectra are summarized in Table 3.5. A tendency similar to the structures of peptides was observed. These results indicate that the formation of  $\beta$  sheet structure is favored by poly(VE)<sub>3</sub>VG, poly(FE)<sub>3</sub>FG and poly(FQ)<sub>3</sub>FG.

For poly(AE)<sub>3</sub>AG, spectra were also measured for the solutions in HFIP at different concentrations in order to investigate the effect of the concentration of polypeptide on the secondary structures. In the spectrum of poly(AE)<sub>3</sub>AG in HFIP at higher concentration,  $\beta$  sheet was detected due to assignment with a positive cotton

**Table 3.5.** Dominant structures of polypeptides in various solvent determined using CD spectroscopy

<b>Polypeptide</b>	<b>In H<sub>2</sub>O</b>	<b>In HFIP/H<sub>2</sub>O=1/1</b>	<b>In HFIP</b>
poly(AE) <sub>3</sub> AG	Random coil	-	Random coil $\beta$ sheet / random coil*
poly(VE) <sub>3</sub> VG	NM	$\beta$ sheet	Random coil
poly(LE) <sub>3</sub> LG	NM	$\alpha$ helix / random coil	Random coil / $\alpha$ helix
poly(LQ) <sub>3</sub> LG	NM	$\alpha$ helix / random coil	Random coil / $\alpha$ helix
poly(FE) <sub>3</sub> FG	NM	$\beta$ sheet	Random coil
poly(FQ) <sub>3</sub> FG	NM	NM	$\beta$ sheet

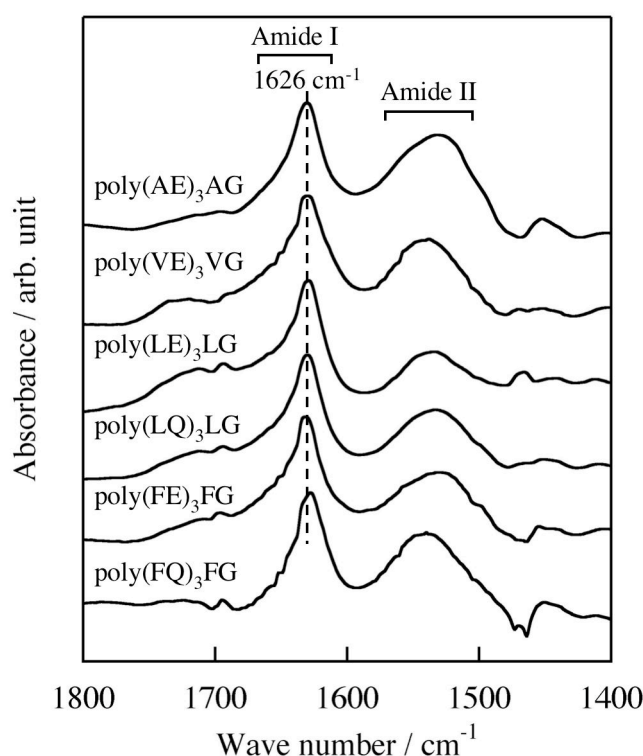
NM: Not measurable, -: Not measured, \*at high concentration  
A: Alanine, V: Valine, L: Leucine, F: Phenylalanine  
E: Glutamic acid, Q: Glutamine



**Figure 3.3.** CD spectra of polypeptides.      ..... : in H<sub>2</sub>O,  
 — : in H<sub>2</sub>O/HFIP, - - - - : in HFIP, - · - · - : in HFIP at 5 mg/mL  
 HFIP: 1,1,1,3,3,3-hexafluoro-2-propanol, A: Alanine, V: Valine, L: Leucine,  
 F: Phenylalanine, E: Glutamic acid, Q: Glutamine

band at 197 nm and a negative cotton band at 217 nm, although random coil was detected at lower concentration. These results indicate that poly(AE)<sub>3</sub>AG formed mainly random coil whereas it can form  $\beta$  sheet structure at higher concentrations such as 5 mg/mL even in HFIP.

As the secondary structures of polypeptides shown above are the structures in solution, their structures in the polypeptide films were investigated using FT-IR and CD spectroscopy. Figure 3.4 shows the FT-IR spectra of the polypeptide films. The two absorption bands located at 1626 and 1550 cm<sup>-1</sup> were assigned to the amide I ( $\nu$ C=O) and amide II ( $\delta$ N-H) stretches, respectively. The strong peak at 1626 cm<sup>-1</sup> in amide I band was attributed to the  $\beta$  sheet structure [9]. This result implies that polypeptides form  $\beta$  sheet structures in the films.



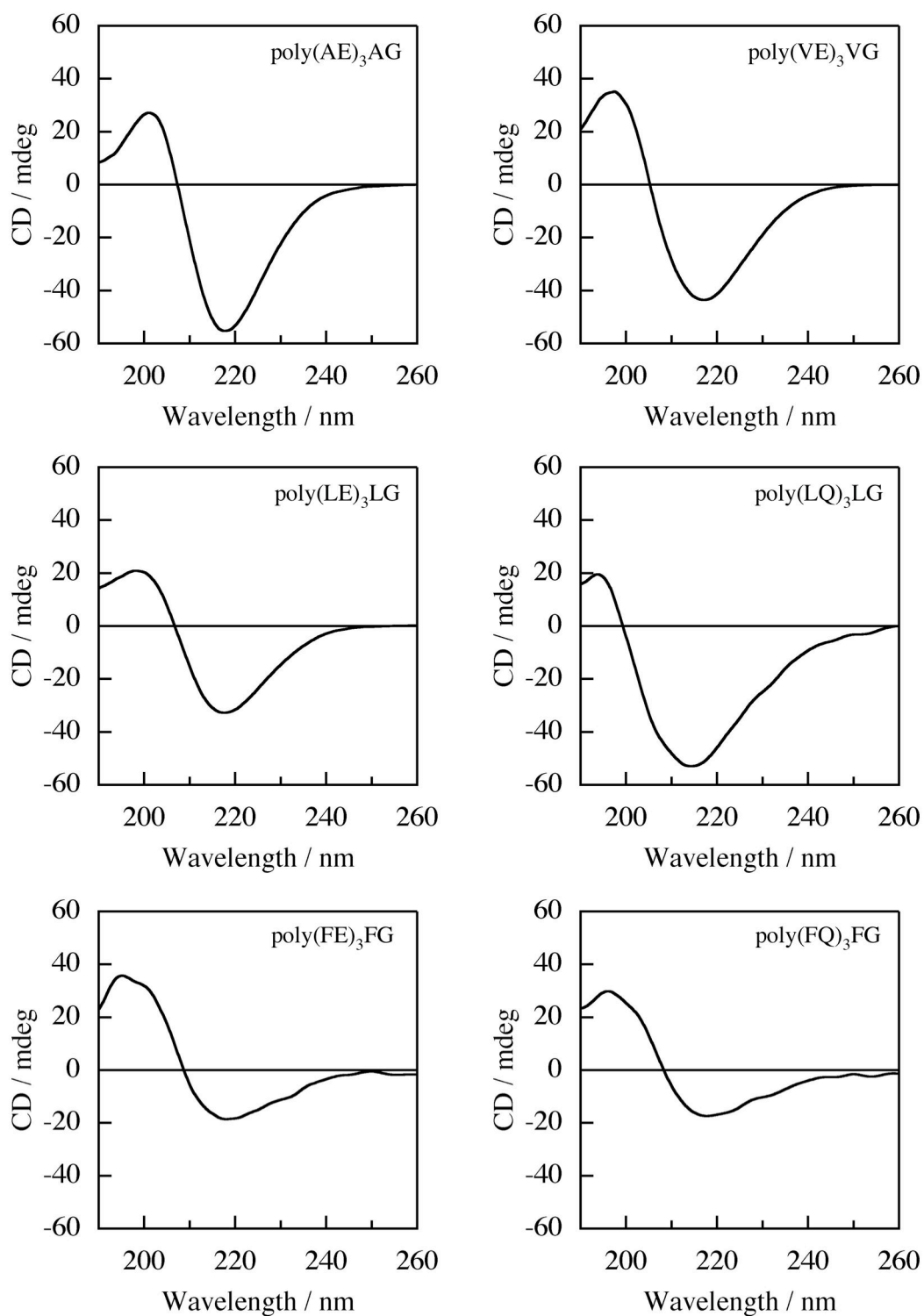
**Figure 3.4.** FT-IR spectra of polypeptide films.  
A: Alanine, V: Valine, L: Leucine, F: Phenylalanine  
E: Glutamic acid, Q: Glutamine

Figure 3.5 shows the CD spectra of polypeptide films. All polypeptide films contained mainly  $\beta$  sheet structure characterized by a positive cotton band around 197 nm and a negative cotton band around 217 nm. It should be noted that the intensity of positive cotton bands in the spectra for poly(VE)<sub>3</sub>VG, poly(FE)<sub>3</sub>FG and poly(FQ)<sub>3</sub>FG was higher than that for the other polypeptides. It suggests that the content of  $\beta$  sheet in films of poly(VE)<sub>3</sub>VG, poly(FE)<sub>3</sub>FG and poly(FQ)<sub>3</sub>FG was higher than that in the other polypeptide films.

**Table 3.6.** Dominant structures of polypeptide films determined using CD and FT-IR spectroscopy

<b>Polypeptide</b>	<b>Secondary structure</b>
poly(AE) <sub>3</sub> AG	$\beta$ sheet
poly(VE) <sub>3</sub> VG	$\beta$ sheet
poly(LE) <sub>3</sub> LG	$\beta$ sheet
poly(LQ) <sub>3</sub> LG	$\beta$ sheet
poly(FE) <sub>3</sub> FG	$\beta$ sheet
poly(FQ) <sub>3</sub> FG	$\beta$ sheet

A: Alanine, V: Valine, L: Leucine, F: Phenylalanine  
E: Glutamic acid, Q: Glutamine



**Figure 3.5.** CD spectra of polypeptide films.  
A: Alanine, V: Valine, L: Leucine, F: Phenylalanine  
E: Glutamic acid, Q: Glutamine

The polypeptide films were soaked in 1.5SBF for 7 days to evaluate the abilities to form hydroxyapatite on their surface. The evaluation results are summarized in Table 3.7. After soaking in 1.5SBF for 7 days, hydroxyapatite formation was not observed on poly(AE)<sub>3</sub>AG and poly(VE)<sub>3</sub>VG films because the films were dissolved during the exposure to 1.5SBF. The other polypeptide films remained even after soaking for 7 days. Hydroxyapatite formation was observed on poly(LE)<sub>3</sub>LG and poly(FE)<sub>3</sub>FG film surfaces whereas not on poly(LQ)<sub>3</sub>LG and poly(FQ)<sub>3</sub>FG. These 4 kinds of polypeptide films were, therefore, soaked in 1.5SBF for various periods and characterized using SEM and thin-film XRD.

Figure 3.6 shows SEM images of poly(LE)<sub>3</sub>LG, poly(LQ)<sub>3</sub>LG, poly(FE)<sub>3</sub>FG and poly(FQ)<sub>3</sub>FG films before and after soaking in 1.5SBF for various periods.

**Table 3.7.** Hydroxyapatite formation on polypeptide films after soaking in 1.5SBF for 7d

<b>Polypeptide</b>	<b>Apatite formation</b>
poly(AE) <sub>3</sub> AG	Dissolved
poly(VE) <sub>3</sub> VG	Dissolved
poly(LE) <sub>3</sub> LG	+
poly(LQ) <sub>3</sub> LG	-
poly(FE) <sub>3</sub> FG	+
poly(FQ) <sub>3</sub> FG	-

+: Apatite formation was observed.

- : Apatite formation was not observed.

A: Alanine, V: Valine, L: Leucine, F: Phenylalanine

E: Glutamic acid, Q: Glutamine



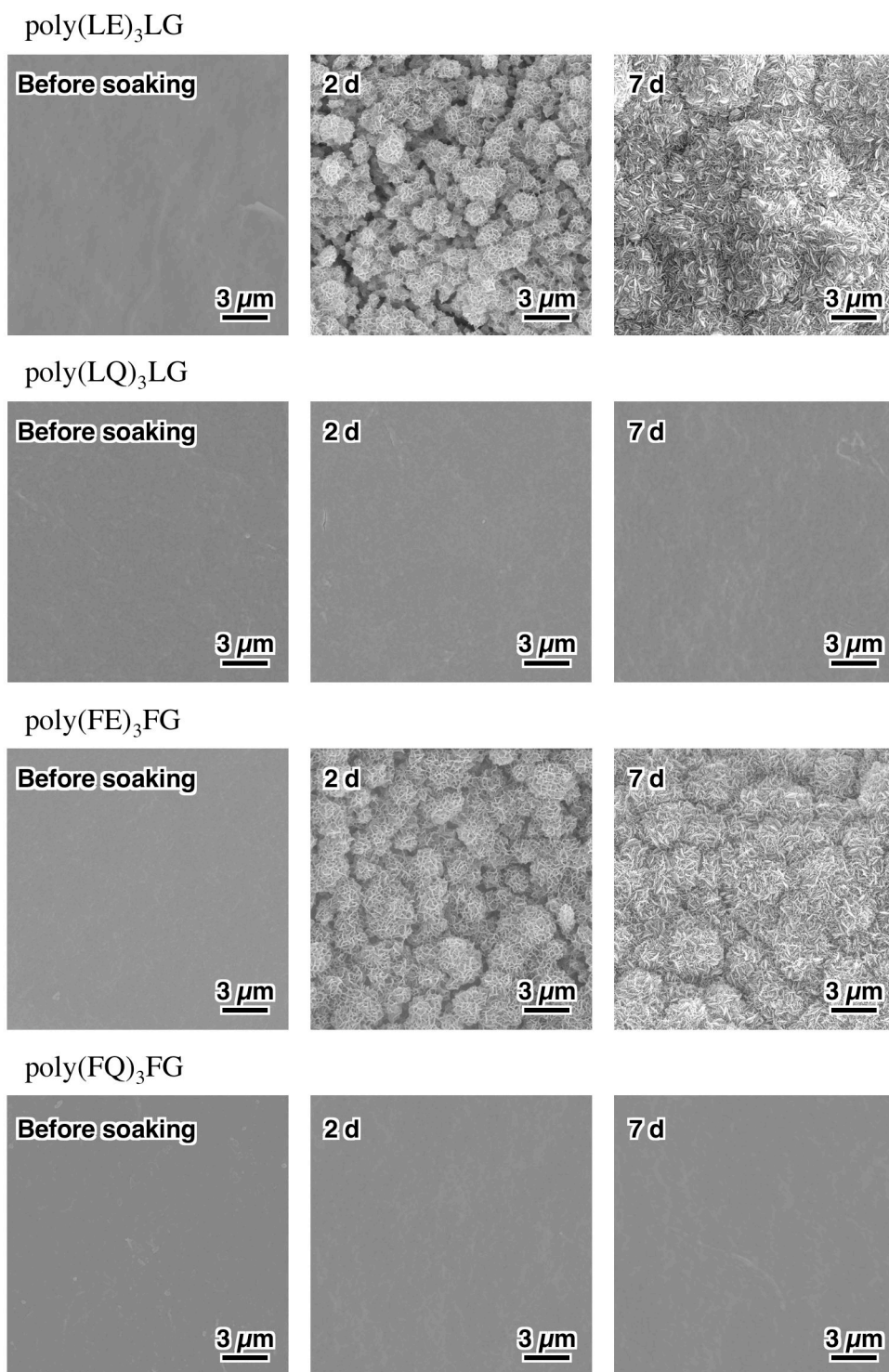


**Figure 3.6.** SEM images of the surfaces of polypeptide films before and after soaking in 1.5SBF for various periods.

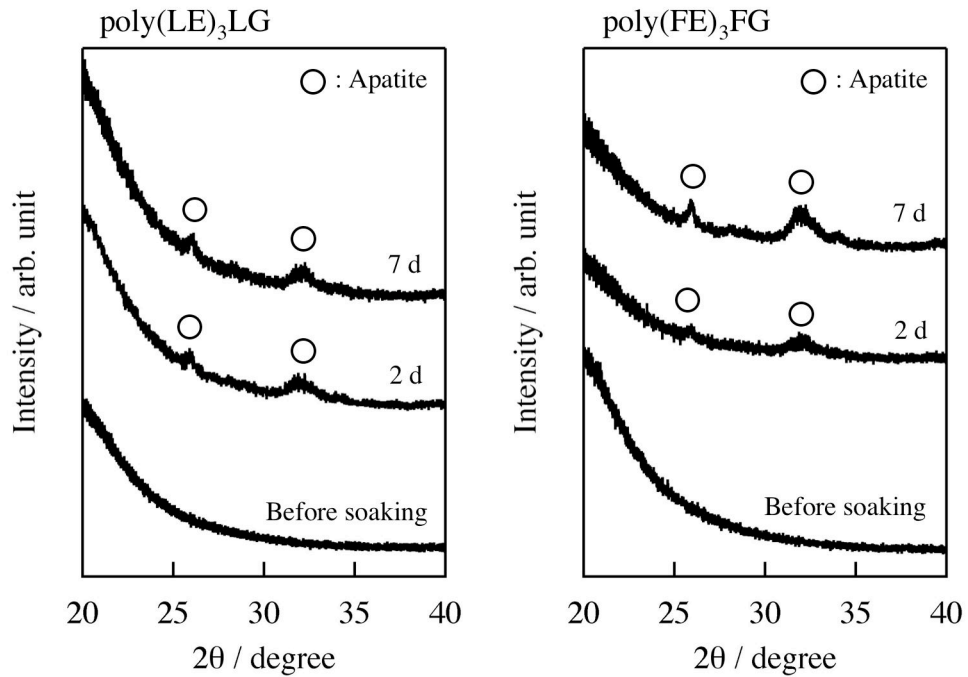
L: Leucine, F: Phenylalanine, E: Glutamic acid, Q: Glutamine



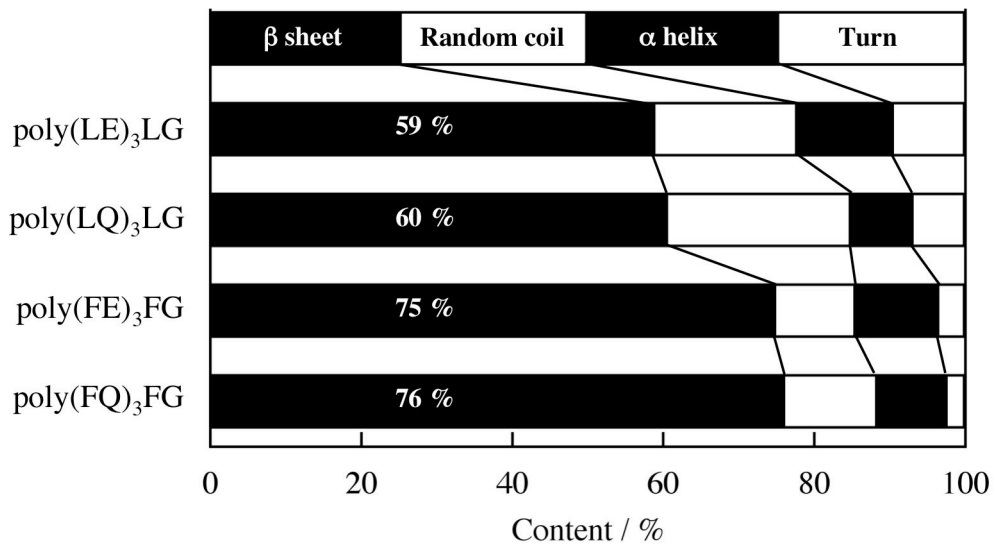
Depositions consisting of fine particles were observed on the surfaces of poly(LE)<sub>3</sub>LG and poly(FE)<sub>3</sub>FG films after soaking in 1.5SBF for the periods more than 2 days. This morphology is similar to that of hydroxyapatite crystals observed on bioactive glasses soaked in SBF [10,11]. On the surfaces of poly(LQ)<sub>3</sub>LG and poly(FQ)<sub>3</sub>FG films, no changes were observed.

Figure 3.7 shows XRD patterns of the surfaces of poly(LE)<sub>3</sub>LG and poly(FE)<sub>3</sub>FG films before and after soaking in 1.5SBF for various periods. Broad peaks that could be assigned to hydroxyapatite were detected around  $2\theta = 26$  and  $32^\circ$  for the samples after soaking in 1.5SBF for the periods of more than 2 days. Additionally, the intensity of peaks assigned to hydroxyapatite for poly(FE)<sub>3</sub>FG films after soaking in 1.5SBF was larger than that for poly(LE)<sub>3</sub>LG films though the difference was quite small. These results suggest that the thickness of the hydroxyapatite layer on poly(FE)<sub>3</sub>FG film was larger than that on poly(LE)<sub>3</sub>LG film.

Contents of secondary structures in the polypeptide films were calculated using the secondary structure analysis software equipped with the CD spectrometer. As Figure 3.8 shows, polypeptides with leucine residues contained about 60% of  $\beta$  sheet and polypeptides with phenylalanine residues contained about 75% of  $\beta$  sheet. The higher content of  $\beta$  sheet in poly(FE)<sub>3</sub>FG film may result in hydroxyapatite formation on poly(FE)<sub>3</sub>FG film more than poly(LE)<sub>3</sub>LG film.



**Figure 3.7.** TF-XRD patterns of the surfaces of polypeptide films before and after soaking in 1.5SBF for various periods.  
 A: Alanine, V: Valine, L: Leucine, F: Phenylalanine  
 E: Glutamic acid, Q: Glutamine



**Figure 3.8.** Contents of secondary structures in polypeptide films.  
 L: Leucine, F: Phenylalanine, E: Glutamic acid, Q: Glutamine

Figure 3.9 shows the contact angles of water on poly(LE)<sub>3</sub>LG, poly(LQ)<sub>3</sub>LG, poly(VE)<sub>3</sub>FG and poly(FQ)<sub>3</sub>FG films. The contact angles on poly(LE)<sub>3</sub>LG, poly(LQ)<sub>3</sub>LG and poly(FQ)<sub>3</sub>FG films were 20.5, 40.7 and 37.6 degree respectively. The contact angle on the poly(VE)<sub>3</sub>FG film was not measurable because the film came off immediately after exposure to water.

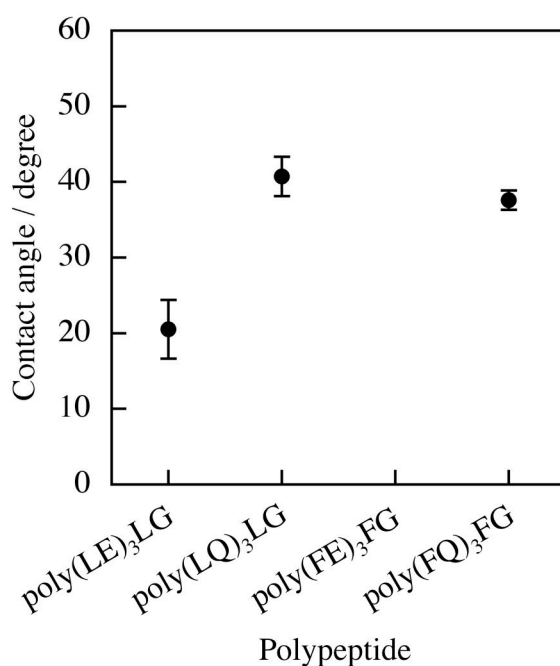


**Figure 3.9.** Contact angles of water on polypeptide films.  
A: Alanine, V: Valine, L: Leucine, F: Phenylalanine  
E: Glutamic acid, Q: Glutamine

#### 4. Discussion

To obtain peptides with a  $\beta$  sheet structure, 6 kinds of peptides with alternating polar/nonpolar amino acid residues were synthesized. Only two peptides of (VE)<sub>3</sub>VG and (FE)<sub>3</sub>FG contained predominantly  $\beta$  sheet structure while the other peptides contained a random coil and/or a  $\alpha$  helix structures under an environment

existing water. These results relate to the preferences of amino acids for  $\alpha$  helix and  $\beta$  sheet shown on Table 3.1. The existence of random coil structure in  $(AE)_3AG$ ,  $(LE)_3LG$  and  $(LQ)_3LG$  might be attributed to the instability of  $\alpha$  helix because the peptides composed of only 8 amino acid residues. They might be also attributed to the mismatching of the sequence to the  $\alpha$  helical repeat. The alternating sequence of the peptide matches the structural repeat of  $\beta$  strand with successive side chains pointing up-down while the sequence that a nonpolar residue is contained every three or four residues matches the  $\alpha$  helical repeat [3]. Therefore, the sequences of peptides of  $(AE)_3AG$ ,  $(LE)_3LG$  and  $(LQ)_3LG$  are suitable for formation of  $\beta$  sheet rather than  $\alpha$  helix.

The dominant structures of all peptides in HFIP were random coil. The increase of HFIP resulted in an inhibition of hydrogen-bonding formation that stabilizes  $\alpha$  helix and  $\beta$  sheet structures. The peptides,  $(VE)_3VG$  and  $(FE)_3FG$ , have  $\beta$  sheet structure even under the condition with HFIP. This indicates that  $(VE)_3VG$  and  $(FE)_3FG$  exceedingly favor to form  $\beta$  sheet structure. The same tendency was observed in structures of polypeptides.

The results of FT-IR and CD measurements for polypeptide films indicate that polypeptides in all films predominantly contained  $\beta$  sheet. The structures of polypeptides containing valine and phenylalanine in solutions remained even after film formation, while the structures of polypeptides containing alanine and leucine was changed from random coil or  $\alpha$  helix to  $\beta$  sheet. These phenomena can be explained by both the preferences on amino acids for  $\alpha$  helix and  $\beta$  sheet and the alternate sequence that favors the formation of  $\beta$  sheet. The polypeptides containing alanine and leucine can form  $\alpha$  helix because they do not have bulky side chains. These polypeptides, therefore, form  $\alpha$  helix and/or random coil that are stabilized by

mainly intramolecular hydrogen bonds, in the dilute solutions, rather than  $\beta$  sheet that are stabilized by mainly intermolecular hydrogen bond. These polypeptides may, however, form  $\beta$  sheet in concentrated solutions because of their alternate sequences. In the process of film formation, the polypeptide solution was concentrated and probably resulted in the formation of  $\beta$  sheet in the film. The results of CD spectroscopy of poly(AE)<sub>3</sub>AG in HFIP at different concentrations of 0.3 or 5 mg/mL support this hypothesis to form  $\beta$  sheet in the process of film formation.

From the results of SEM and XRD analysis of polypeptide films containing either phenylalanine or leucine and both before and after soaking in 1.5SBF, it is obvious that poly(LE)<sub>3</sub>LG and poly(FE)<sub>3</sub>FG have an ability to induce hydroxyapatite nucleation in 1.5SBF. In addition, the nucleation ability of poly(FE)<sub>3</sub>FG was higher than that of poly(LE)<sub>3</sub>LG owing to the higher content of  $\beta$  sheet structure. This demonstrates that polypeptide dominant with  $\beta$  sheet provide effective surfaces for hydroxyapatite nucleation.

The peptides with alternating polar/nonpolar amino acid residues allow  $\beta$  strands to have a successive arrangement of side chains pointing above and below the peptide chains, and the  $\beta$  strands aggregate to form  $\beta$  sheet structure. Two different structures of  $\beta$  sheet can be built up. The first structure is nonpolar side chains equally distributed on both sides of the sheet: nonpolar side chains are directed towards one side, those of the other chain towards the other. The second structure is that all nonpolar side chains point to the same side of the sheet.

Brack *et al.* [12] investigated the conformation of poly(Val-Lys). They showed that the alternating polypeptide formed the second type of  $\beta$  sheet in which the positively charged amino groups arranged themselves on one side of a  $\beta$  sheet under a condition existing of salts and the hydrophobic faces in the  $\beta$  sheets

aggregate to form a bi-layer structure. Poly(LE)<sub>3</sub>LG and poly(FE)<sub>3</sub>FG synthesized in this study may also form  $\beta$  sheet structure with a surface on which the carboxyl groups in glutamic acid are arranged. The reasonableness of this explanation for such a structure was confirmed using molecular mechanical calculation. Figure 3.10 shows computed  $\beta$  sheet structures of (LE)<sub>3</sub>LG and (FE)<sub>3</sub>FG that were calculated by InsightII program (Molecular Simulations Inc.) using Amber force field parameters. Both peptides can form the  $\beta$  sheet structure that has polar and nonpolar face, though carboxyl groups contained in the peptides showed a tendency to repel each other electrostatically.

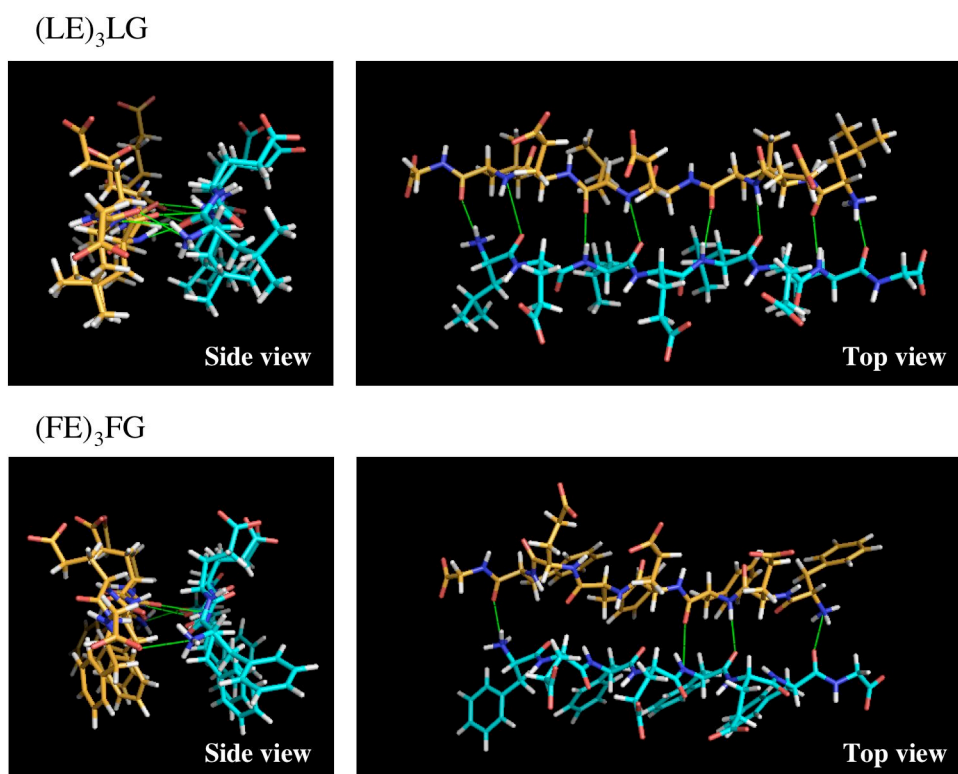


**Figure 3.10.** Computed  $\beta$  sheet structures in water of (LE)<sub>3</sub>LG and (FE)<sub>3</sub>FG. Green line indicates hydrogen bond.  
L: Leucine, F: Phenylalanine, E: Glutamic acid  
The graphics were drawn using the PyMol Molecular Graphics System (DeLano Scientific)

The results of contact angle measurement demonstrated that the surface of polypeptide films was rich in carboxyl groups. The arranged carboxyl groups due to  $\beta$  sheet formation may partly exist on polypeptide films.

The results suggest that ordered and concentrated carboxyl groups are important for effective nucleation of hydroxyapatite. A hydroxyapatite nucleation is initiated by incorporation of  $\text{Ca}^{2+}$  ion into carboxyl groups [13]. The ordered and concentrated carboxyl groups allow  $\text{Ca}^{2+}$  ions to bind effectively to the carboxyl groups. Figure 3.11 shows the diagrams of  $\text{Ca}^{2+}$  ion bindings to the carboxyl groups. One  $\text{Ca}^{2+}$  ion incorporates with two carboxyl groups cooperatively in one case, and one  $\text{Ca}^{2+}$  ion incorporates with one carboxyl group in another case. In both cases, the existence of carboxyl groups in appropriate distance and high flexibility in arrangement of carboxyl groups are essential for effective incorporation of  $\text{Ca}^{2+}$  ion.

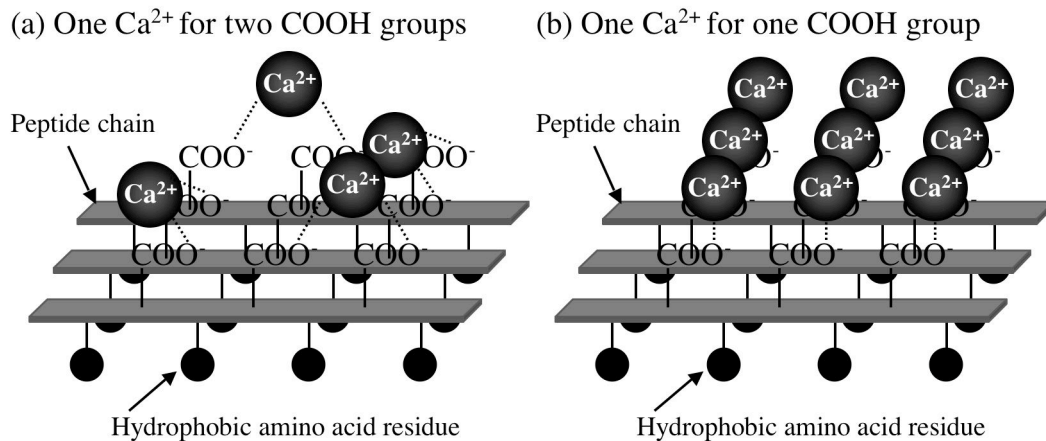


**Figure 3.11.** Schematic diagram of  $\text{Ca}^{2+}$  binding onto poly( $\text{LE}$ )<sub>3</sub>LG or poly( $\text{FE}$ )<sub>3</sub>FG films.

The ordered and concentrated carboxyl groups may also be templates for hydroxyapatite nucleation. Figure 3.12 shows the crystal structure of hydroxyapatite reported by Young *et al.* [14]. Comparison of the periodicity of  $\text{Ca}^{2+}$  ions in hydroxyapatite with the periodicity of carboxyl groups in polypeptides shows that there was a good matching along the  $c$  axis of hydroxyapatite, as shown in Figure 3.13.

A similar phenomenon on mineralization in shell nacre was also reported [15]. Shell nacre is composed of calcium carbonate and organic matrices, repeated domains of aspartic acid and neutral amino acid have  $\beta$  sheet. The resulting arrangement of aspartic acid enables  $\text{Ca}^{2+}$  ion to bind to carboxyl group, and there is a geometric matching between the periodicity of  $\text{Ca}^{2+}$  ions in calcium carbonate and the matrix periodicity. Considering these points of view, the ordered carboxyl groups play an important role in nucleation of calcium carbonate and it is essential even in nucleation of hydroxyapatite.

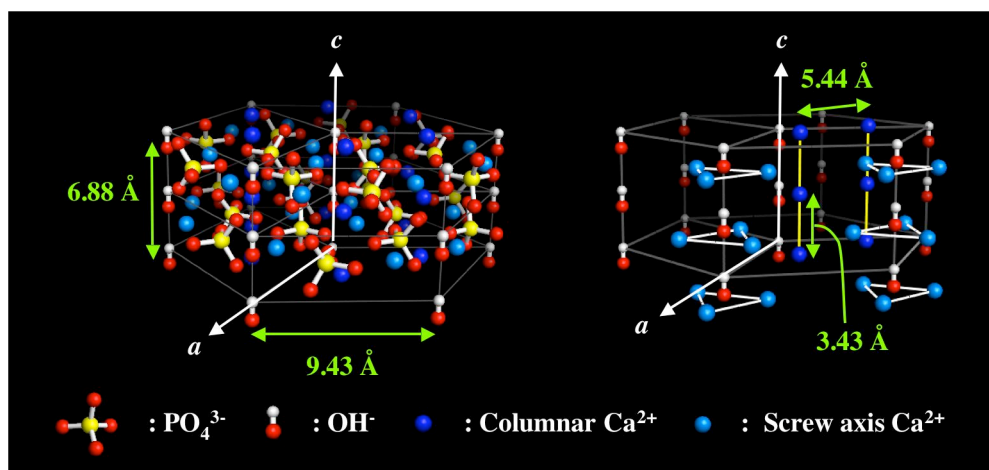
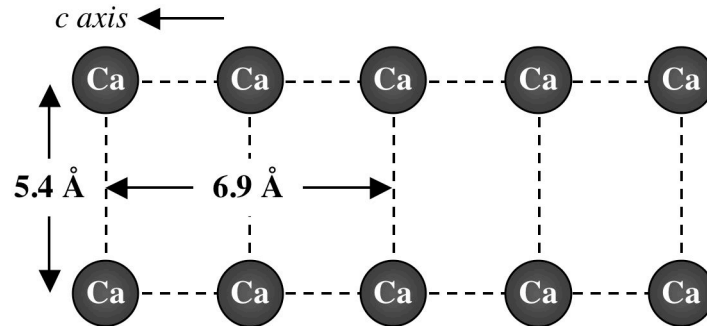


**Figure 3.12.** Crystal structure of hydroxyapatite. [14]  
From inorganic crystal structure database (<http://icsdweb.fiz-karlsruhe.de/>).  
The graphics were drawn using the PyMol Molecular Graphics System.



(a) Periodicity of columnar  $\text{Ca}^{2+}$  in hydroxyapatite crystal



(b) Periodicity of carboxyl groups in polypeptides

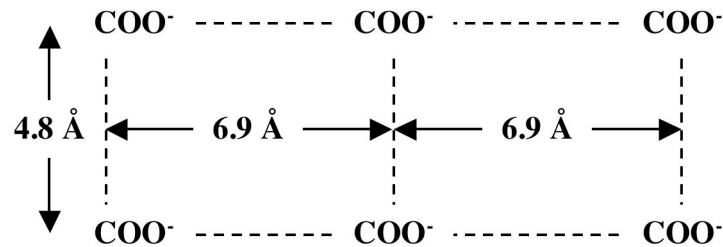


**Figure 3.13.** Structural matching between hydroxyapatite and polypeptides synthesized in this study.

## 5. Conclusion

The polypeptide films that contains a  $\beta$  sheet structure, poly(LE)<sub>3</sub>LG and poly(FE)<sub>3</sub>FG, can effectively induce hydroxyapatite deposition on its surface in a solution mimicking body environment. The induction of hydroxyapatite nucleation can be attributed to the concentrated and ordered carboxyl groups on the surface of the polypeptide films.

## References

- [1] Abe Y, Kokubo T, Yamamuro T. Apatite coating on ceramics, metals and polymers utilizing a biological process. *J Mater Sci Mater Med* 1990;1:233-238.
- [2] Tanahashi M, Yao T, Kokubo T, Minoda M, Miyamoto T, Nakamura T, Yamamuro T. Apatite coating on organic polymers by a biomimetic process. *J Am Ceram Soc* 1994;77:2805-2808.
- [3] Xiong H, Buckwalter BL, Shieh HM and Hecht MH. *Proc Natl Acad Sci USA* 1995;92:6349-6353.
- [4] Levitt M. Conformational preferences of amino acids in globular proteins. *Biochemistry* 1978;17:4277-4284.
- [5] Brahms S, Brahms J. Determination of protein secondary structure in solution by vacuum ultraviolet circular Dichroism. *J Mol Biol* 1980;138:148-178.
- [6] Madison V, Schellman J. Optical activity of polypeptides and proteins. *Biopolymers* 1972;11:1041-1076.
- [7] Greenfield N, Fasman GD. Computed circular dichroism spectra for the evaluation of protein conformation. *Biochemistry* 1969;8:4108-4116.
- [8] Townend R, Kumosinski TF, Timasheff SN, Fasman GD, Davidson B. The circular dichroism of the  $\beta$ -structure of poly-L-lysine. *Biochem Biophys Res Comm* 1966;23:163-169.
- [9] Miyazawa T, Blout ER. The infrared spectra of polypeptides in various conformations: amide I and II bands. *J Am Chem Soc* 1961;83:712-719.
- [10] Ohtsuki C, Kokubo T, Takatsuka K, Yamamuro T. Compositional

- dependence of bioactivity of glasses in the system CaO-SiO<sub>2</sub>-P<sub>2</sub>O<sub>5</sub>: Its *in vitro* evaluation. J Ceram Soc Japan (Seramikkusu Ronbunshi) 1991;99:1-6.
- [11] Ohtsuki C, Kushitani H, Kokubo T, Kotani S, Yamamuro T. Apatite formation on the surface of Ceravital-type glass-ceramic in the body. J Biomed Mater Res 1991;25:1363-1370.
- [12] Brack A, Orgel LE.  $\beta$  structure of alternation polypeptides and their possible prebiotic significance. Nature;256:383-387.
- [13] Takadama H, Kim HM, Kokubo T, Nakamura T. Mechanism of apatite formation induced by silanol groups: TEM observation. J Ceram Soc Japan 2000;108:118-121.
- [14] Sudarsanan K, Young RA. Significant precision in crystal structural details: holly springs hydroxyapatite. Acta Cryst 1969;B25:1534-1543.
- [15] Mann S. Molecular recognition in biomineralization. Nature 1988;332:119-124.

## ***General Summary***

This thesis has described an investigation into hydroxyapatite formation on a polypeptide under a condition mimicking body environment. As a polypeptide, silk proteins were primary focused on to examine their ability to induce heterogeneous nucleation of hydroxyapatite because of their composition of amino acids and secondary structure. Hydroxyapatite formation on silk proteins was investigated in a solution mimicking body fluid. Furthermore, some polypeptides were designed on the basis of the results obtained from hydroxyapatite formation on the silk proteins. Hydroxyapatite formation on synthetic polypeptides was also investigated in a solution mimicking body fluid. The content of each chapter is summarized as follows.

In Chapter 1, two types of fabric made from raw silk fiber and degummed silk fiber were examined. These fibers have different proteins on their surfaces: the raw silk fiber contains sericin, whereas the degummed silk fiber contains fibroin. Deposition of hydroxyapatite particles was observed on the fabric made from raw silk after soaking in 1.5SBF, but not on normal silk. This suggests that the surface consisting of sericin produces effective sites for hydroxyapatite formation in a biomimicking solution, such as 1.5SBF. This was confirmed by examining the hydroxyapatite-forming ability of sericin film under the same conditions. Sericin

## *General Summary*

---

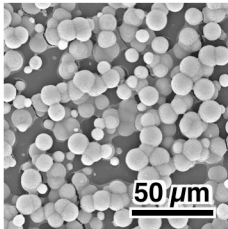
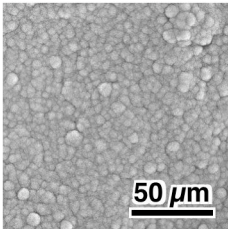
contains a high concentration of acidic amino acids such as glutamic acid and aspartic acid. They provide a surface rich in carboxyl groups, which induced heterogeneous nucleation of hydroxyapatite. Hydroxyapatite formation on fabric made from raw silk was significantly accelerated by prior treatment with  $\text{CaCl}_2$  solution of concentration 1 M ( $=\text{kmol}\cdot\text{m}^{-3}$ ) or more.

In Chapter 2, sericin films with different structures were prepared and hydroxyapatite formation on their surfaces in 1.5SBF was investigated. Only the sericin film with a high content of  $\beta$  sheets showed hydroxyapatite-forming ability in 1.5SBF. This result demonstrated that hydroxyapatite nucleation on sericin was governed by the arrangement as well as the existence of carboxyl groups.

In Chapter 3,  $\beta$  sheet-forming polypeptides containing carboxyl groups were designed according to the findings in Chapter 2. Four kinds of polypeptide films containing  $\beta$  sheet structures were successfully synthesized. Both poly(LE)<sub>3</sub>LG and poly(FE)<sub>3</sub>FG deposited hydroxyapatite on their surfaces in 1.5SBF within 2 days. In these polypeptides, all carboxyl groups in glutamic acids are speculated to point above the  $\beta$  sheet. Concentrated and/or ordered carboxyl groups on polypeptide film surfaces may provide effective sites for heterogeneous nucleation of hydroxyapatite in 1.5SBF.

Table 1 summarizes the results obtained in Chapters 2 and 3. Comparing the content of carboxyl groups between sericin and the synthetic polypeptide, the synthetic polypeptide contains approximately twice as many carboxyl groups as sericin. Nevertheless, the ability of the synthetic polypeptide to form hydroxyapatite was much higher than that of sericin: the whole surface of synthetic polypeptide film was covered with hydroxyapatite layer after soaking in 1.5SBF for 2 day whereas sericin film was not covered completely even after soaking for 7 days. Only

**Table 1.** Comparison between the results of sericin and synthetic polypeptide films

	Sericin	Synthetic polypeptide
Content of acidic amino acid	20 mol%	38 mol%
Content of $\beta$ sheet structure	42 %	60 %, 75 %
Apatite formation on the films after soaking in 1.5SBF	7 d soaking 	2 d soaking 

two or three carboxyl groups can exist close together on the sericin film surface because of the amino acid sequence of sericin. In contrast, more carboxyl groups can exist orderly on the surface of the synthetic polypeptide film than on the sericin film surface. A highly ordered arrangement of carboxyl groups on the surface of the synthetic polypeptide film produces a considerable improvement in the ability to form hydroxyapatite in 1.5SBF.

These results gave us an idea to design an organic polymer to prepare hydroxyapatite-organic polymer hybrids. Namely, the carboxyl groups arranged by  $\beta$  sheet structure effectively induce the heterogeneous nucleation of hydroxyapatite. The arrangement of carboxyl groups with dimensions larger than the critical nucleus of hydroxyapatite may also enable the nucleus to grow easily to form a hydroxyapatite layer.

## *General Summary*

---

The hydroxyapatite layer formed in a biomimicking solution, such as 1.5SBF, is composed of carbonate-containing hydroxyapatite with low crystallinity, which has similar characteristics to the hydroxyapatite in natural bone. Such carbonate-containing hydroxyapatite, so-called bone-like apatite, shows a high biological affinity when implanted into bone defects and can achieve tight bonding to living bone. Hydroxyapatite-organic polymer hybrids fabricated through the present method is, therefore, expected to show direct bonding to living bone, and such hybrid materials can be useful for the application of, not only bone substitutes, but also of scaffolds for tissue engineering.

In the preparation of hydroxyapatite-organic polymer hybrids, it is key engineering to find an organic polymer that can effectively induce heterogeneous nucleation of hydroxyapatite in a biomimicking solution. This thesis demonstrates the importance of the arrangement of the functional groups as well as the existence of the functional groups that induce heterogeneous nucleation of hydroxyapatite. This finding provides us with a guideline to design a novel organic polymer for preparing hydroxyapatite-organic polymer hybrids.

# ***Publication List***

---

The present thesis, “Hydroxyapatite deposition on polypeptide under a condition mimicking body environment”, is based on the following publications.

## ***Chapter 1***

Deposition of bone-like apatite on silk fiber in a solution that mimics extracellular fluid

A. Takeuchi, C. Ohtsuki, T. Miyazaki, H. Tanaka, M. Yamazaki, M. Tanihara, 2003, *J. Biomed. Mater. Res.*, **65A**, 283-289.

## ***Chapter 2***

Heterogeneous nucleation of hydroxyapatite on protein: structural effect of silk sericin

A. Takeuchi, C. Ohtsuki, T. Miyazaki, M. Kamitakahara, S. Ogata, M. Yamazaki, Y. Furutani, H. Kinoshita, M. Tanihara, 2005, *J. R. Soc. Interface*, **2**, 373-378.



## Related Publications

Apatite formation on silk sericin in a solution mimicking extracellular fluid

A. Takeuchi, C. Ohtsuki, T. Miyazaki, S. Ogata, M. Tanihara, H. Tanaka, Y. Furutani, H. Kinoshita, 2002, in *Proceedings of 2nd Asian BioCeramics symposium (ABC2002)*, Committee of Asian BioCeramics symposium, pp. 93-96.

Apatite formation on silk fiber in a solution mimicking body fluid

A. Takeuchi, C. Ohtsuki, T. Miyazaki, S. Ogata, M. Tanihara, H. Tanaka, Y. Furutani, H. Kinoshita, 2003, in *Bioceramics, Vol. 15 (Key Engineering Materials Vols. 240-242)*, ed. by B. Ben-Nissan, D. Sher and W. Walsh, Trans Tech Publications Ltd., Switzerland, pp. 31-34.

Effect of sericin coating on biodegradation of porous alpha-tricalcium phosphate

A. Takeuchi, C. Ohtsuki, M. Kamitakahara, S. Ogata, M. Tanihara, T. Miyazaki, M. Yamazaki, Y. Furutani, H. Kinoshita. 2003, in *Archives of BioCeramics Research Vol. 3*, ed. by M. Okazaki, K. Ishikawa, K. Yamashita, Y. Doi and S. Ban, Saga Printing Ltd., Japan, pp. 114-117.

Apatite deposition on silk sericin in a solution mimicking extracellular fluid: effects of fabrication process of sericin film

A. Takeuchi, C. Ohtsuki, M. Kamitakahara, S. Ogata, M. Tanihara, M. Yamazaki, T. Miyazaki, Y. Furutani, H. Kinoshita, 2004, in *Bioceramics, Vol. 16 (Key Engineering Materials Vols. 254-256)*, ed. by M. A. Barbosa, F. J. Monteiro, R. Correia and B. Leon, Trans Tech Publications Ltd., Switzerland, pp. 403-406.

### Control of bioresorption of porous alpha-tricalcium phosphate

T. Miyazaki, C. Ohtsuki, A. Takeuchi, M. Kamitakahara, S. Ogata, M. Tanihara, H. Tanaka, Y. Furutani, H. Kinoshita, 2004, *Transactions of the Materials Research Society of Japan (Trans. MRS-J)*, **29**, 2923-2926.

### Biodegradation of porous alpha-tricalcium phosphate coated with silk sericin

A. Takeuchi, C. Ohtsuki, M. Kamitakahara, S. Ogata, M. Tanihara, T. Miyazaki, M. Yamazaki, Y. Furutani, H. Kinoshita, 2005, in *Bioceramics*, **Vol. 17 (Key Engineering Materials, Vol. 284-286)**, ed. by P. Li, K. Zhang and C. W. Colwell, Jr., Trans Tech Publications Ltd., Switzerland, pp.329-332.

### Apatite formation on synthetic polypeptide with $\beta$ sheet structure in a solution mimicking body environment

A. Takeuchi, C. Ohtsuki, M. Kamitakahara, S. Ogata, M. Tanihara, T. Miyazaki, 2006, in *Bioceramics*, **Vol. 18 (Key Engineering Materials, Vol. 309-311)**, ed. by T. Nakamura, K. Yamashita and M. Neo, Trans Tech Publications Ltd., Switzerland, pp. 489-492.

### Development of novel bioactive PMMA-based bone cement and its *in vitro* and *in vivo* evaluation

S.B. Cho A. Takeuchi, I.Y. Kim, S.B. Kim, C. Ohtsuki, M. Kamitakahara, 2006, in *Bioceramics*, **Vol. 18 (Key Engineering Materials, Vol. 309-311)**, ed. by T. Nakamura, K. Yamashita and M. Neo, Trans Tech Publications Ltd., Switzerland, pp.801-804.

# ***Acknowledgements***

---

The studies in the present thesis were carried out under the direction of Professor Masao Tanihara at the Graduate School of Materials Science, Nara Institute of Science and Technology, Japan.

The author expresses her sincere gratitude to Professor Masao Tanihara and Associate Professor Chikara Ohtsuki at the Graduate School of Materials Science, Nara Institute of Science and Technology, Japan, for their continuing guidance, valuable suggestions, and fruitful discussions through these studies.

The author is sincerely grateful to Professor Jun-ichi Kikuchi and Professor Tadashi Shiosaki at the Graduate School of Materials Science, Nara Institute of Science and Technology, Japan, for their valuable advice.

The author's sincere gratitude also goes to Dr. Shin-ichi Ogata; Dr. Masanobu Kamitakahara, both at the Graduate School of Materials Science, Nara Institute of Science and Technology, Japan; and Dr. Toshiki Miyazaki at the Graduate School of Life Science and Systems Engineering, Kyushu Institute of Technology, Japan, for their support and helpful suggestion.

The author is sincerely grateful to Mr. Masao Yamazaki at the Kyoto Prefectural Institute for Northern Industry, Japan, for providing us with the silk fabrics used in the study of the present thesis and for helpful suggestions, Mr. Hisao Kinoshita at CENTMED Inc., Japan and Mr. Yoshiaki Furutani at PHG Corp., Japan for their helpful suggestions.

The author is sincerely grateful to Dr. Aiko Okamura at the Research Center of Advanced Bionics in National Institute of Advanced Industrial Science and Technology, Japan; Dr. Takahiro Kawai at the Japan Science and Technology Agency, Japan; Dr. Ruth D. Goodridge at Wolfson School of Mechanical &

Manufacturing Engineering, Loughborough University, the United Kingdom; Mr. Taro Kinumoto at the Graduate School of Engineering, Kyoto University, Japan; Ms. Mutsumi Usui and all students in the Laboratory of Biocompatible Materials Science, the Graduate School of Materials Science, Nara Institute of Science and Technology, Japan, for their continuing encouragement, support and helpful suggestions.

A part of the studies in the present thesis were carried out with the support of the Sasagawa Scientific Research Grant from the Japan Science Society and the Foundation for Nara Institute of Science and Technology.

Finally, the author expresses her hearty gratitude to her parents, Mr. Norio Takeuchi, Mrs. Katsuko Takeuchi, and to her sister, Ms. Michiru Takeuchi, for their warm understanding, patience, support and continuing encouragement during the long hours.

March 2006

---

Akari Takeuchi